

THESIS FOR THE DEGREE OF DOCTOR OF PHILOSOPHY

PROBING THE NANO-BIO INTERFACE USING SURFACE BASED
ANALYTICAL TECHNIQUES

RICKARD FROST



Department of Applied Physics

CHALMERS UNIVERSITY OF TECHNOLOGY

Göteborg, Sweden 2012

Probing the Nano-Bio Interface Using Surface Based Analytical Techniques
RICKARD FROST

ISBN 978-91-7385-763-5

© RICKARD FROST, 2012.

Doktorsavhandlingar vid Chalmers tekniska högskola
Ny serie nr 3444
ISSN 0346-718X

Department of Applied Physics
Chalmers University of Technology
SE-412 96 Göteborg
Sweden
Telephone + 46 (0)31-772 1000

Cover:

Wordcloud based on the text in the abstract of this thesis and the abstracts of the appended papers. The size of the words is related to how frequent they occur in the mentioned texts.

Chalmers Reproservice
Göteborg, Sweden 2012

RICKARD FROST

Department of Applied Physics
Chalmers University of Technology

Abstract

In recent years, the use of manufactured nanomaterials has been rapidly increasing in a wide range of application areas. Among others, these areas of application include cosmetics, medicine, clothing, and sporting goods. The small size of nanomaterials offers unique properties that are not possible to obtain by the same material in bulk. Although the use of nanomaterials holds great promises for society, the increased use and production also increases the concern that engineered nanomaterials may have adverse effects on human health or the environment.

Unlike chemical substances, which have a defined structure and mass, nanomaterials need to be described by a large number of descriptors, *e.g.*, size distribution, shape, and composition. In addition, to address possible effects on humans or the environment, it is of great importance to determine how nanomaterials interact with biological matter. Interactions with proteins, cell membranes, and cells may cause protein coronas, cellular uptake, or biocatalytic processes. To fully characterize such interactions there is a strong need for novel analytical techniques or methodologies.

In this thesis, I have investigated how the lipid membrane, one of the most vital structures of a cell, interacts with various types of nanomaterials (*e.g.* polyelectrolyte complexes, graphene oxide, and TiO₂ nanoparticles). The interactions between the model membranes and the nanomaterials have been studied using several complementary surface sensitive techniques. The results have showed conformational changes of polyelectrolyte complexes upon adsorption to the membranes and triggered disintegration of such complexes upon exposure to an acidic or a reducing environment. Furthermore, TiO₂ nanoparticles have been shown to be able to disrupt lipid membranes in a Ca²⁺-mediated mechanism and a novel nanocomposite material, composed of alternating layers of graphene oxide and lipid membranes, has been prepared. In addition, the quartz-crystal microbalance with dissipation monitoring technique (QCM-D) has been explored in studies of intracellular transport processes using living cells. Specifically, pigment translocation in *Xenopus laevis* melanophores, has been shown to generate significant QCM-D responses. By using the described methodology, it is possible to evaluate the nanoparticle design and study how nanomaterials behave at a biological interface or effect specific cellular functions.

Keywords: nanomaterial, cell membrane, supported lipid bilayer, nanomedicine, nanotoxicology, QCM-D, AFM, DPI, melanophores

List of appended papers

This thesis is based on the work contained in the following papers:

- I. Structural rearrangements of polymeric insulin-loaded nanoparticles interacting with surface-supported model lipid membranes**
Frost, R., Grandfils, C., Cerda, B., Kasemo, B., and Svedhem, S
J. Biomaterials and Nanobiotechnology **2**, 180-192, (2011)
- II. Bioreducible insulin-loaded nanoparticles and their interaction with model lipid membranes**
Frost, R., Coué, G., Engbersen, J.F.J., Zäch, M., Kasemo, B., and Svedhem, S.
J. Colloid Interface Sci. **362**, 575-583, (2011)
- III. Graphene Oxide and Lipid Membranes: Interactions and Nanocomposite Structures**
Frost, R., Edman Jönsson, G., Chakarov, D., Svedhem, S., and Kasemo, B.
Nano Lett. **12**, 3356-3362, (2012)
- IV. TiO₂ nanoparticle induced damage in lipid membranes**
Zhao, F., Holmberg, J. P., Frost, R., Abbas, Z., Kasemo, B., Hassellöv, M., and Svedhem, S. *In revision*
- V. Acoustic detection of melanosome transport in *Xenopus laevis* melanophores**
Frost, R., Norström, E., Bodin, L., Christoph Langhammer, Sturve, J., Wallin, M., and Svedhem, S. *Submitted*

Publications not included in the thesis

- VI. Pore Spanning Lipid Bilayers on Mesoporous Silica Having Varying Pore Size**
Claesson, M., Frost, R., Svedhem, S., and Andersson, M.
Langmuir **27**, 8974-8982, (2011)
- VII. Characterization of nanoparticle – lipid membrane interactions using QCM-D**
Frost R. and Svedhem S.
Invited chapter accepted for publication in the volume “Cellular and Subcellular nanotechnology: Methods and Protocols” that will be part of the “Methods in Molecular Biology” series edited by John M. Walker, Humana Press (USA), Springer Publishing Group

My contribution to the appended papers

- Paper I. I planned and performed all experimental work apart from the SEM analyses. I had the main responsibility for writing the paper.
- Paper II. I planned and performed all experimental work apart from the polymer synthesis and drug loading efficiency measurements. I had the main responsibility for writing the paper.
- Paper III. I planned and performed all experimental work. I had the main responsibility for writing the paper.
- Paper IV. I performed the AFM analyses and wrote related parts of the paper.
- Paper V. I was responsible for the experimental design and performed all QCM-D experiments and the confocal microscopy analyses. I had the main responsibility for writing the paper.

List of abbreviations

AFM	atomic force microscopy
DLS	dynamic light scattering
DPI	dual polarization interferometry
ECHA	european chemicals agency
EC	european commission
EPR	enhanced permeability and retention
EU	european union
HI	human insulin
LB	langmuir-blodgett
LS	langmuir-schaeffer
NP	nanoparticle
OECD	organization for economic co-operation and development
PAA	poly(amido amine)
PBS	phosphate buffered saline
PEC	polyelectrolyte complex
PEG	polyethylene glycol
POEPC	1-palmitoyl-2-oleyl- <i>sn</i> -glycero-3-ethylphosphocholine
POPC	1-palmitoyl-2-oleyl- <i>sn</i> -glycero-3-phosphocholine
POPG	1-palmitoyl-2-oleoyl- <i>sn</i> -glycero-3-phosphoglycerol
POPS	1-palmitoyl-2-oleyl- <i>sn</i> -glycero-3-phospho-L-serine
PTC	phenylthiocarbamide
QCM-D	quartz crystal microbalance with dissipation monitoring
REACH	Registration, Evaluation, Authorization and Restriction of Chemical substances
RES	reticuloendothelial system
SAR	structure-activity relationship
SEM	scanning electron microscopy
SLB	supported lipid bilayer
TE	transverse electric
TM	transverse magnetic
WPMN	Working Party on Manufactured Nanomaterials

“Lack of patience in small matters can create havoc in great ones.”

- Chinese proverb

Table of contents

1 INTRODUCTION	1
1.1 AIM OF THESIS.....	3
2 NANOMATERIALS.....	5
2.1 DEFINITION.....	5
2.2 OCCURRENCE.....	6
2.2.1 Graphene oxide.....	6
2.2.2 TiO ₂ nanoparticles	7
2.2.3 SiO ₂ nanoparticles.....	8
2.3 ACTIVITIES FOR RISK ASSESSMENT	9
2.3.1 OECD	9
2.3.2 EU.....	11
3 NANOPARTICLE-BASED DRUG DELIVERY	13
3.1 NANOFORMULATIONS FOR INCREASED BIOAVAILABILITY	13
3.2 NANOPARTICLE DESIGNS FOR PASSIVE AND ACTIVE TARGETING	14
3.1 COMMON CLASSES OF NANOPARTICLES FOR DRUG DELIVERY	16
3.1.1 Liposomes	16
3.1.2 Polymeric nanoparticles	16
3.1.3 Magnetic nanoparticles.....	17
4 THE CELL MEMBRANE – A BIOLOGICAL INTERFACE	19
4.1 BIOLOGICAL BARRIERS AND UPTAKE OF NANOPARTICLES.....	19
4.1.1 The cell membrane	19
4.1.2 The lipid molecule.....	20
4.1.3 Cellular uptake of nanoparticles.....	21
4.2 MEMBRANE MODEL SYSTEMS.....	23
4.2.1 Liposomes	23
4.2.2 Supported lipid bilayers	24
4.2.3 Langmuir-Blodgett films.....	25
4.3 FORCES AT THE NANO-BIO INTERFACE.....	25
4.4 FROM MEMBRANE MODELS TOWARDS WHOLE CELL ANALYSES	28
5 EXPERIMENTAL TECHNIQUES.....	31
5.1 NANOPARTICLE SIZE AND ZETA POTENTIAL MEASUREMENTS	31
5.2 QCM-D.....	32
5.2.1 QCM-D and cells.....	35
5.3 AFM.....	36
5.4 DPI.....	37
5.5 REFLECTOMETRY.....	39
6 SUMMARY OF THE APPENDED PAPERS	41
6.1 BRIEF SUMMARY OF PAPERS.....	41
6.2 EXPERIMENTAL PLATFORM FOR NANOMATERIAL – LIPID MEMBRANE INTERACTIONS	42
6.2.1 Insulin-loaded drug carriers (Paper I and II)	42
6.2.2 Graphene oxide (Paper III).....	47
6.2.3 TiO ₂ nanoparticles (Paper IV)	50
6.3 MONITORING OF INTRACELLULAR TRANSPORT BY QCM-D (PAPER V)	51
6.3.1 Effects of SiO ₂ nanoparticle exposure (Additional results).....	55
7 CONCLUDING REMARKS AND FUTURE PERSPECTIVES	57
8 ACKNOWLEDGEMENTS.....	59
9 REFERENCES	61

Introduction

We have always been surrounded by natural nanometer-sized particles (nanoparticles, NPs), *e.g.* dust and ash, without taking any notice of it.¹ Foreign matter in the body is in most cases efficiently removed by the reticuloendothelial system. However, during the last century, particle pollution due to human activities (anthropogenic) has increased dramatically, mainly because of the industrial development and combustion-based engine transportation, and it has been shown that particle pollution may cause severe health disorders. More recently, during the last decades, the boom of nanotechnology has become another significant contributor to the large-scale production of various nanomaterials.

The physico-chemical properties of engineered nanomaterials are unique and make the materials useful for many technological and medical applications. Today, nanomaterials are used in many commercial products including clothing, sunscreens, cosmetics, and adhesives (see Chapter 2 for a definition and an overview of nanoparticle occurrence and application). In the field of nanomedicine, the merging of nanotechnology and medicine, nanomaterial-based formulations are employed for administration of drugs (common nanodrug designs are described in Chapter 3).² Nano-sized drug carriers are predicted to greatly improve drug administration during the 21st century.³ By reformulating existing drugs into a nano-sized carrier to improve their pharmacokinetics, *i.e.* the fate of the drug after administration, is a cost efficient alternative to the development of novel drugs. One way to achieve this is to use a carrier that allow drugs to more efficiently be delivered across biological barriers, and even targeted to the diseased tissue.⁴ This rapidly developing methodology holds a great promise because of its potential to control (i) the biodegradation, (ii) the bioavailability and (iii) the potential side effects of a drug in a positive way.

The increased use and production volumes of engineered nanomaterials, increases the likelihood of people coming in contact with such materials. As a consequence there is a significant concern that nanomaterials may have adverse effects on the human health and/or the environment.⁵ Such lessons have been learned in the cases of asbestos⁶, and air pollution in general^{7, 8}. Asbestos is a term for a group of fibrous minerals that are known to cause lung cancer, and the more rare cancer called mesothelioma. These minerals also increase the risk of autoimmune diseases. Regarding air pollution, it is well established that inhaled particles can have adverse health effects, such as cardiovascular diseases or respiratory illnesses. However, the health effects due to particle inhalation vary greatly with the type of particles that are present in the air. The field of nanotoxicology, where the toxic properties of nanomaterials are assessed, first emerged when nanomaterials were already used in industrial processes and products.⁹

The development of novel nanomaterials has been growing exponentially and it is not possible, or even reasonable, to fully characterize the toxic effects of all emerging materials. One strategy to overcome this problem is to extensively characterize a selection of common types of nanomaterials in order to define structure-activity relationships that in turn may be used to predict the properties of similar materials. The knowledge obtained on ultrafine particles (<100 nm) of dust and air pollutants provides a starting point to predict possible health effects of engineered nanomaterials.^{10, 11} The major challenge when addressing the toxic properties of nanomaterials compared to chemical compounds is that there are many more variables to consider. Relevant nanoparticle descriptors include: size, shape, charge, coating, concentration, roughness, agglomeration, aggregation and composition (Figure 1). These various properties distinguish nanotoxicology from classical toxicology, where a mass based dose-metric is used.

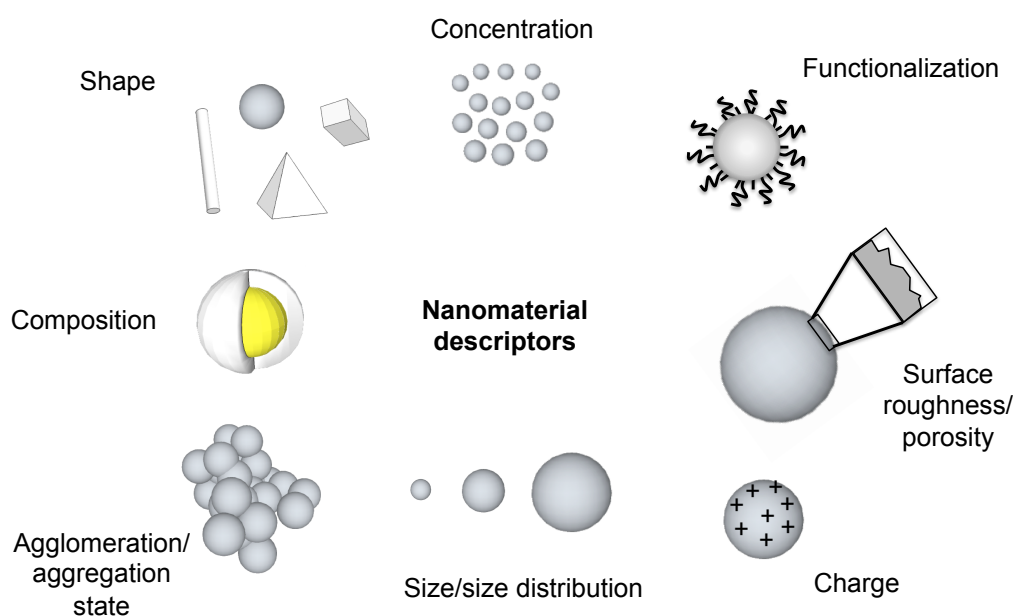


Figure 1. Overview of physico-chemical descriptors of nanomaterials.

To further characterize nanomaterials, it is of great importance to learn how such materials interact with living systems. It has been shown that nano-sized materials can translocate across cell membranes, and reach the cytoplasm, either through active or passive mechanisms. In fact, nanoparticles have even been reported to enter the cell nucleus.¹² Nanoparticles for drug delivery often need to overcome different biological barriers, *e.g.* mucus layers or cell membranes, to reach their intended target. On the other hand, nanomaterials that are engineered for other purposes may cause negative effects if taken up by a cell. For the nanoparticle to enter the cell, it must pass the plasma membrane. This biological barrier, which is very efficient and complex, encapsulates the whole cell and partition the intracellular environment from the extracellular. The core structure of the plasma membrane is the phospholipid bilayer, a structure that consists of amphiphilic lipid molecules. Apart from the outer cell membrane, many intracellular organells, *e.g.* mitochondria and nucleus, are also confined by a phospholipid bilayer. The cell membrane control intracellular homeostasis

through selective transport mechanisms across the membrane, processes that are essential for cell survival. Because of this, the cell membrane is a sensitive target for possible effects of nanoparticles. The cell membrane is further described in Chapter 4 together with common model systems thereof.

In order to fully exploit the benefits of nanomaterials in a responsible way, it is of great interest to better understand in what way different nanomaterials interact with biological barriers, specifically the cell membrane.¹³⁻¹⁵ One of the strategies chosen in this thesis is to use a well defined model system of the native cell membrane (see further Chapter 4). Other researchers have also adopted the use of model systems of the cell membrane to investigate their interactions with nanomaterials.^{13, 15-17} There are different approaches to engineer membrane model systems, and plain lipid bilayers are attractive due to their low degree of complexity.¹⁸ Lipid membranes are readily formed, from dispersed liposomes, on hydrophilic supports such as SiO₂.¹⁹ Supported lipid membranes can be studied by a variety of different surface sensitive analytical techniques.^{16, 20} The analytical techniques used in this work are described in Chapter 5. A second strategy to address cell membrane interactions was used to assess nanoparticle interactions with complex model systems, *i.e.* living cells, and to probe direct or indirect effects of nanomaterial exposure.

1.1 Aim of thesis

The aim of the work presented in this thesis has been to establish a platform for in depth studies of the nano-bio interface using surface sensitive analytical techniques. The two main foci have been to study the interactions between various nanomaterials and (i) well defined supported lipid membranes (schematically illustrated in Figure 2), or (ii) living cells using acoustic sensing.

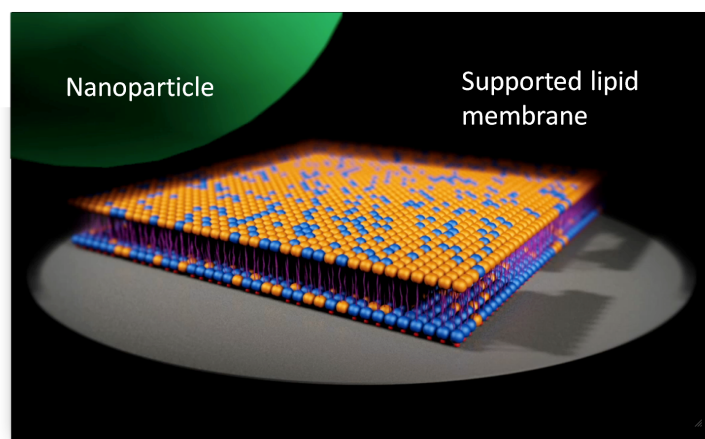


Figure 2. Schematic illustration of a nanoparticle approaching a supported lipid membrane consisting of two types of lipid molecules.

2

Nanomaterials

2.1 Definition

The prefix “nano”, which originate from the Greek “nanos” signifying “dwarf”, has become a very popular label within science. Words like nanoantenna, nanoporous and nanoarrays have become common in the scientific literature although they are not widely established. However, more and more nano words enter the dictionaries. At present the words nanometer, nanosecond, and nanotechnology are included in the Swedish Academy Dictionary. Nano denotes one billionth (10^{-9}), *i.e.* one nanometer (nm) is one billionth of a meter. In newspaper reporting the use of “nano” is common. In a recent linguistic analysis of Swedish newspaper articles, covering a 22-year period, close to 400 different words containing “nano” were identified.²¹

For the purpose of safety regulation and legislation it is of great importance to define what should be classified as a nanomaterial. It has become evident, due to the ongoing global debate, that it is not a trivial task to come up with a definition that captures all nanomaterials. Often a nanomaterial is defined as a material with at least one dimension in the range of 1-1000 nm. However, in other definitions the size of at least one dimension is limited to 1-100 nm. This smaller limit is motivated by changes in physical properties of some materials that occur when reaching this size regime. For example, the surface atoms of nano-sized particles have less neighbors and hence a lower binding energy compared to atoms in the bulk material, this results in a lower melting temperature for the nanoparticles.²² Thus, it has been argued that rather than basing a definition on size, it should be based on changes in material physical properties.

In October 2011 the European commission adopted a recommendation of the definition of a nanomaterial.²³ According to that definition a nanomaterial means:

“A natural, incidental or manufactured material containing particles, in an unbound state or as an aggregate or as an agglomerate and where, for 50 % or more of the particles in the number size distribution, one or more external dimensions is in the size range 1 nm-100 nm.”

“In specific cases and where warranted by concerns for the environment, health, safety or competitiveness the number size distribution threshold of 50 % may be replaced by a threshold between 1 and 50 %.”

In December 2014 this definition will be reviewed, focusing on whether the given number size distribution threshold should be increased or decreased. Similarly, in nanomedicine, it is important to define the field and what a nanomedicine is. One could claim that most common medicines are nanomedicines since small molecules and proteins are in the nanometer size

range. Again, there exist many different definitions. One of them is given by the European Technology Platform on nanomedicine and reads as follows.²⁴

“Nanomedicine is the application of nanotechnology to health. It exploits the improved and often novel physical, chemical, and biological properties of materials at the nanometric scale.”

In the given definition size dimensions of 1-1000 nm are included. One motivation for this is that in the area of medicine, nanotechnology is used to interact with cells and tissues. For this purpose materials larger than 1-100 nm is utilized.²⁴

2.2 Occurrence

As was already mentioned in the introduction, nanomaterials have always been around since there are several natural sources of these materials. Natural sources that produce large quantities of particles, and have the potential to affect tremendously large areas, are dust storms, forest fires, and volcano eruptions. These events generate high concentrations of particulate matter (including nanoparticles) that may cause adverse health effects. Another major natural source of nanoparticles are the seas and oceans across the world. When water evaporates and when waves generate water drops in the atmosphere, sea salt aerosols are formed. The sizes of these particles range from 100 nm to several microns. However, there are no adverse health effects associated with sea salt aerosols.¹

In addition to the natural sources, anthropogenic nanomaterials constitute another major source. Nanomaterials are created in combustion processes, of *e.g.* fuel and coal, as well as in the chemical industry. Such by-products of human activities have been present for a very long time. When it comes to deliberate production and use of nanomaterials the number of produced nanoparticle types and applications areas have increased tremendously the last decades. However, already the Romans used metal nanoparticles to color glass. One famous example is the Lycurgus cup that was made in the 4th century.²⁵ Today nanomaterials are commonly used in many commercial products including cosmetics, medicines, clothing, sporting goods, tires, and sunscreens. Although the number of products is rapidly increasing, there are attempts to make an inventory of all nanotechnology-based products on the market.²⁶ In the studies that form the basis of this thesis, a few selected nanomaterials have been included. These materials, apart from the drug carriers, are described in some detail in the following subchapters. Nanoparticle-based drug delivery, including polymeric drug carries, is described in Chapter 3.

2.2.1 Graphene oxide

In recent years, after the observation and characterization of exfoliated graphene by Novoselov *et. al.* in 2004²⁷, graphene based materials have become an intense area of research and the materials are explored for numerous applications.^{28, 29} Materials based on graphene include, in addition to graphene itself, graphene oxide, carbon nanotubes and fullerenes. These materials may

also be functionalized to further tune their properties. One strategy is to combine the extraordinary properties of graphene and its derivatives with other materials in composites.³⁰ Materials that successfully have been used in graphene based composites include, for example, inorganic nanostructures³¹⁻³³, polymers³⁴ and biomolecules³⁵. Applications of such composites include batteries³³, supercapacitors³², photovoltaic devices³¹, and sensing platforms³⁵. Due to the increasing use of these materials it was of great interest to study a graphene based material with respect to its lipid membrane interactions. Graphene is a hydrophobic material and needs to be functionalized with hydrophilic groups to be soluble in aqueous environments. Hence, in our experiments we chose to work with graphene oxide due to its water solubility. Simplistically, graphene oxide is a graphene sheet with hydroxyl, and epoxy functional groups on the basal plane of the sheet. Carbonyl groups are also present, mainly as carboxylic acids along the border of the sheet. These functional groups can be seen as reactive handles that may be used to produce functionalized graphene based materials.

The most common route to produce large quantities of graphene oxide begins with the oxidation of graphite to graphite oxide. In this process, the sp^2 -hybridization structure of the stacked graphene sheets in graphite is converted to sp^3 . This conversion makes the atomic structure of graphene oxide distorted resulting in an increased surface roughness. Hence, the oxidation process increases the distance between the stacked sheets of graphene oxide. This process also facilitates delamination of graphite oxide into individual sheets of graphene oxide by sonication.²⁹ The thickness of a graphene oxide monolayer has been determined by AFM to 1.6 nm. However, due to the intrinsic surface roughness, the thickness of bi- and trilayers are 2.6 nm and 3.6 nm respectively.³⁶ Although oxidized graphene is an insulator it is possible reduce the material to restore the electrical properties. For the production of large quantities of graphene from graphene oxide there is a need to develop a reduction method that minimizes the residual oxygen content.

2.2.2 TiO₂ nanoparticles

TiO₂ is commonly used as a nanomaterial due to its many important application areas, *e.g.* photocatalysis^{37, 38}, water purification³⁹ and solar energy conversion⁴⁰. In addition, due to the high refractive index of TiO₂, it is often used as a white pigment in paints and other commercial products.⁴¹ It should be noted that the white color is obtained from larger TiO₂ NPs or agglomerates of smaller ones. If the size of the NPs is reduced, the color is lost. TiO₂ NPs have the ability to absorb and block ultraviolet light, a property that is utilized in sunscreens. In recent years, the size of the TiO₂ NPs in sunscreens has been reduced to obtain a transparent layer when applied to the skin. Since sunscreens often are applied before bathing or swimming they are a significant source of TiO₂ NP contamination to the water compartment. Naturally, due to the photocatalytic properties of TiO₂, the NPs used in sunscreens are coated with a different material, usually SiO₂, Al₂O₃, or ZrO₂.⁴² Potential emissions of TiO₂ NPs from sunscreens, and other sources, has been conducted using particle flow analysis.⁴³

There exist three different crystal structures of TiO₂, namely brookite, anatase, and rutile. These structures have different properties.⁴⁴ Due to the many

applications and large production volume TiO₂ nanoparticles is included in the OECD list of nanomaterials to be thoroughly evaluated (see section 2.3.1).

2.2.3 SiO₂ nanoparticles

As early as in the 1860s, Thomas Graham prepared silica colloids. However, the silica technology proceeded slowly and the early silica sols (colloidal silica dispersed in liquid) were only produced at low concentrations, were not stable over time, and did not have reproducible properties.⁴⁵ It took almost a century to overcome these issues and to develop production methods of silica sols for use in commercial products. Today colloidal silica is produced in large quantities and used in numerous applications, where the use as retention aid in papermaking is likely the largest. In papermaking, a slurry of pulp is turned into a solid sheet of paper through a dewatering process where the cellulose fibers need to be retained in the paper. The efficiency of this process is significantly increased by the use of colloidal silica together with charged polymers as a retention aid. Another large application of colloidal silica is the use as an additive to cement and concrete. By addition of silica nanoparticles, the cement hardens very fast due to a rapid consumption of the available water. This process increases the strength of the final product. Additionally, SiO₂ nanoparticles are also used in *e.g.* coatings, solid electrolytes, and polishing agents.⁴⁵ For the same reasons as for TiO₂ nanoparticles, *i.e.* the many areas of applications and the current large scale production volumes, SiO₂ nanoparticles are also included in the OECD list of nanomaterials to be thoroughly evaluated (see section 2.3.1).

2.3 Activities for risk assessment

When discussing risk assessment it is important to be aware of the related concepts hazard, exposure and risk. The hazard, of the material in this case, is related to the intrinsic properties that may cause an adverse effect. Exposure is a measure of to what extent a hazard is present, while risk (= hazard x exposure) is the probability for an adverse effect to occur (Figure 3). In the following sections, the activities for the risk assessment of nanomaterials within OECD and EU are described.



Figure 3. Risk = hazard x exposure

2.3.1 OECD

OECD is an intergovernmental organization with representatives from 34 developed countries in Europe (including Sweden), North and South America, Asia and the Pacific region. In addition to these countries, the European Commission is also represented in OECD. In this organization the member countries discuss issues of mutual concern, co-ordinate policies and respond to international problems in a unified manner. In September 2006, the OECD council established the Working Party on Manufactured Nanomaterials (WPMN) to address the implication of manufactured nanomaterials on the human health and the environmental safety. This working party aims to ensure that the approach to hazard, exposure and risk assessment of manufactured nanomaterials is of an internationally harmonized standard. WPMN bring together more than 100 experts, partly from OECD member countries but also from non-member countries and international organizations. To address issues regarding manufactured nanomaterials WPMN heads the following projects.⁴⁶

- OECD database on manufactured nanomaterials to inform and analyze EHS (environment, health and safety) research activities.
- Safety testing of a representative set of manufactured nanomaterials.

- Manufactured nanomaterials and test guidelines.
- Co-operation on voluntary schemes and regulatory programs
- Co-operation on risk assessment
- The role of alternative methods in nanotoxicology
- Exposure measurement and exposure mitigation
- Environmentally sustainable use of manufactured nanomaterials

One of these projects involves safety testing of manufactured nanomaterials. In this project a representative set of manufactured nanomaterials has been chosen and all materials will be thoroughly investigated. The concept of this project is that testing a certain set of nanomaterials can derive much valuable information regarding the safety of nanomaterials in general and the assessment methods. In this way, the understanding of what intrinsic properties of the nanomaterials that affects the human health and the environment may be significantly increased. The project is implemented in two stages. First, a list of representative manufactured nanomaterials and a specific set of endpoints were agreed upon. The nanomaterials that were selected (Figure 4) are all on the market or close to be introduced on the market.⁴⁷

Fullerenes (C60)	Silver nanoparticles	Aluminum oxide	Silicon dioxide	Gold nanoparticles
Single-walled carbon nanotubes	Iron nanoparticles	Cerium oxide	Dendrimers	
Multi-walled carbon nanotubes	Titanium dioxide	Zinc oxide	Nanoclays	

Figure 4. The manufactured nanomaterials selected by WPMN. The table of nanomaterials should be viewed as a “snapshot in time” as materials could be added or removed depending on the current use and production of nanomaterials.

In the second stage, the OECD Sponsorship Program for the Testing of Manufactured Nanomaterials has been launched. In this program, the selected nanomaterials will be tested with respect to human health and environmental safety. For each of the included nanomaterials about 60 pre-decided endpoints should be determined. The selected endpoints belong to the following areas.⁴⁷

- Nanomaterial information/identification (9 endpoints)
- Physical-chemical properties and material characterization (17 endpoints)
- Environmental fate (15 endpoints)
- Environmental toxicology (6 endpoints)
- Mammalian toxicology (9 endpoints)
- Material safety (3 endpoints)

For each nanomaterial to be tested, a lead sponsor, *i.e.* one of the countries involved in WPMN, is responsible for conducting or coordinating the tests necessary to determine the endpoints. For some nanomaterials, there is a joint lead sponsorship. The process of conducting the tests is in progress and will most likely last for several years ahead.

2.3.2 EU

The EU policy on the development of nanotechnologies is that it should be “integrated, safe and responsible”.⁴⁸ This standpoint includes reviewing and adapting EU laws, monitoring safety issues and to be engaged in dialogue with national authorities and other stakeholders. In the European commission (EC), which is one of the main institutions within the EU, there are several activities regarding nanotechnology. These activities are distributed among different departments (DGs, Directorates-General) dealing with policies in various areas, *e.g.*, health and consumers, research, education, or environment. An important task for the EC has been, and still is, to dedicate EU research funding to areas addressing safety aspects of nanotechnologies. Under the sixth and seventh framework programme (FP 6 and FP7), thirty research projects regarding the safety of nanomaterials, with a total founding of 80 million EURO, was included.⁴⁹ To maximize the synergy between these project the European Nanosafety Cluster has been formed. The EC also supply knowledge to international bodies working with related risk assessment, *e.g.* the OECD.

In 2004 there was a communication from the EC entitled “Towards a European strategy for nanotechnology”.⁴⁸ In this communication, the need to identify and address safety concerns (both real and perceived) at an early stage, is highlighted. The following year, an action plan for Europe regarding nanosciences and nanotechnologies was adopted.⁵⁰ One of the main areas in this action plan regards the safety aspects of nanomaterials. Later, the action plan has been followed up with two implementation reports, in which the progress was reported.^{51, 52}

To ensure that sufficient information regarding the hazards of chemical substances is available, the REACH (Registration, Evaluation, Authorization and Restriction of Chemical substances) regulation was adopted in 2007. By the means of REACH, the human health and the environment will be better protected since the intrinsic properties of substances will be identified at an early stage. According the REACH regulation, there is a great responsibility of the industry to provide safety information on the substances they manufacture or use. This information must be reported to the European Chemicals Agency (ECHA) where it is stored in a central database. However, although nanomaterials are covered by the definition of substances in REACH, the regulation is not well adapted to such materials. The main reasons for this being that only substances produced in quantities of more than one tonne per year need to be registered and a chemical safety report must be produced when the quantities exceed 10 tonnes per year.⁵³

Nanoparticle-based drug delivery

The merging of nanotechnology and medicine is commonly referred to as Nanomedicine.⁵⁴ It is a rapidly expanding field of research including many different applications, such as drug delivery systems⁵⁵, contrast agents for *in vivo* imaging⁵⁶, sensor platforms for *in vitro* diagnostics⁵⁷, as well as medical implants and scaffolds for tissue engineering⁵⁸. The expectations on the field of Nanomedicine are high in terms of *e.g.* improved therapies and diagnostics. However, nanotechnology is often associated with unrealistic futuristic scenarios. For example, in Michael Crichton's novel *Prey* nanorobots develop their own intelligence and become a large threat. For this reason it is important to distinguish between the objectives that could be realized for the benefit of common health within a reasonable timescale and plain fiction. The great potential of this area arises from the fact that the length scale of the nanomaterials coincides with the length scale of the smallest functional entity in the cell, the proteins. The engineering of functional materials in the nano scale is predicted not only to provide a more effective interaction with living cells but also to reach intracellular targets. For this purpose, nanomedicines need to compromise biological barriers, processes that may give rise to unexpected toxicities. Because of this, it is also of great importance to assess the safety of nano-sized drug carriers.⁴⁹

3.1 Nanoformulations for increased bioavailability

Many of the applications within Nanomedicine are based on the use of nano-sized particles.⁵⁹ For example, NPs are designed as drug carriers to protect, target, and release an active substance at the target site, thus minimizing adverse systemic effects.⁶⁰ The bioavailability of the drug, *i.e.* the fraction of the delivered dose that reaches the circulation system, depends on the specific properties of the drug and the chosen route of administration. There are several different routes to administer drugs, *e.g.* orally, pulmonary, or by injections. Some are more convenient than others and because of this they are more often preferred. By the use of drug carriers it could potentially be possible to alter the route of administration when developing new formulations. It is also preferred to administer the smallest possible dose to obtain the desired effect since the risk of adverse side effects is decreased. By targeted drug delivery, a local high dose of the drug at its intended site of action can be reached while healthy tissues in other areas of the body are exposed at lower concentrations. This lowers the risk of adverse side effects tremendously. An additional advantage of small doses is that drug molecules in general and biopharmaceuticals in particular, are expensive to prepare. If only a small amount of the drug were needed the cost could be kept low.

Human insulin, a hormone that removes excess glucose from the blood and that is used in the treatment of diabetes mellitus, is a common model protein in the development of NP formulations. When formulating this hormone, the aim is

to reach a high bioavailability using non-parental routes of administration. Ideally, the outcome of research performed on NP formulations of human insulin could be used when formulating other biomolecular drug molecules. Diabetes mellitus is a family of diseases in which the blood glucose levels are too high. It is a chronic condition that affects a tremendous number of people worldwide every year. Since insulin was first extracted from the pancreas in 1921 by Banting and Best, huge efforts have been made to administer the hormone in a convenient way for the treatment of the disease. The most common way to administer insulin is through subcutaneous injections and despite the inconvenience for the patients, no alternative routes of administrations have been successful so far. As early as in 1924 the first studies on inhaled insulin were published⁶¹ and since then pulmonary and other non-parental routes of administration, such as transdermal, nasal, oral, and rectal have been investigated.^{62, 63} In January 2006, Exubera[®], an advanced method by Pfizer/Nektar Therapeutics based on recombinant insulin for inhalation, was approved by both the European and the American drug agencies (EMA and FDA). Although it was the first product of its kind on the market it was withdrawn in October 2007 due to low market acceptance.⁶⁴ Other devices for inhaled insulin has reached phase III in clinical trials. One such product was AERx[®] iDMS developed by Aradigm Corporation and Novo Nordisk. However, Novo Nordisk stopped all investigations on inhaled insulin shortly after Pfizer announced that Exubera[®] was being withdrawn from the market. Due to the ease of administration and patient compliance, oral delivery of human insulin has also gained large focus. Materials that have been used to formulate insulin for oral delivery include polymeric hydrogels⁶⁵, polymeric solid nanoparticles⁶⁶ and liposomes⁶⁷. Polyelectrolyte complexes (PECs) have also been prepared for non-invasive insulin delivery.⁶⁸⁻⁷⁰ In this work several different insulin loaded PECs have been studied with respect to their lipid membrane interactions.

3.2 Nanoparticle designs for passive and active targeting

Nanoparticulate drug formulations have various degree of functionalization depending on the drug to be administered and the chosen route of administration. With respect to their functionalities, drug carriers are often referred to as the first, second or third generation. A construct prepared from a plain nano sized carrier and a drug, is referred to as the first generation of NPs for drug delivery (Figure 5A). In more advanced designs, the nanodrug is functionalized with a targeting entity (Figure 5B and C). This entity is commonly an antibody, part of an antibody, a peptide, or an aptamer. The targeting molecules then direct the drug to a specific organ or a cell type that express the ligand to the targeting molecule on the cell surface. For example, tumor biomarkers such as epidermal growth factor (EGF) receptors have been successfully targeted in cancer treatments.⁷¹

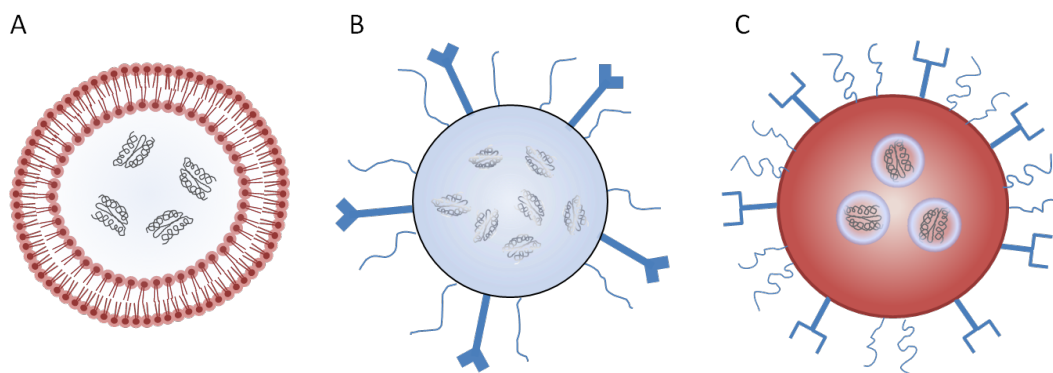


Figure 5. The first, second, and third generation of drug carriers. (A) The first generation consists of a carrier and its drug load. (B) The second generation the drug carriers are functionalized, *e.g.* with shielding and/or targeting entities. (C) The third generation drug carriers contain several payloads with different targets.

When targeting solid tumors it is possible to reach a high local concentration of NPs in the tumor without a specific targeting moiety, due to the enhanced permeability and retention (EPR) effect. The EPR effect relates to the leakiness of the vascular tumor tissue,⁷² and provides a mechanism for passive targeting. The targeting of the drug to the diseased tissue rather than having an even distribution it in the entire body increases the efficacy of the drug and reduces the risk of adverse side effects. At the site of action, the release of the active substance could either be passive or initiated by different methodologies depending on the nature of the NP. An active drug release could be achieved by heating absorbing particles through irradiation with ultrasound or light⁷³ (which could also be the actual therapy) or by enzymatic cleavage⁷⁴. In the latter case the carrier must be engineered so that it dissociates or releases the drug in any other way as a response to a specific enzyme present at the target site. A third approach to an active drug release is to use the local environment in tumors as a trigger, since tumor tissue normally has a lower pH compared to healthy tissue.⁷⁵

When the particle is functionalized with a targeting molecule and/or an active release mechanism they are referred to as the second generation of NPs for drug delivery (Figure 5B). The NPs could also be functionalized in additional ways. For example, it has been shown that pegylation of NPs can significantly prolong their residence time within the bloodstream (a necessary step in the direction towards so called stealth drugs).^{76, 77} In this way, the foreign material is protected from opsonization and further elimination/degradation by the reticuloendothelial system (RES). When toxic substances are to be delivered, the body should be protected from the substance in a similar manner.

Even more advanced approaches aim at multifunctional particles combining therapy and diagnostics (theranostics), such as magnetic particles which can be used both as contrast agents in MR imaging, and local treatment by the application of an external magnetic field. NPs which belong to the third and, so far, most advanced generation of NPs for drug delivery have the ability to overcome multiple biological barriers (Figure 5C). For example, particles could have multiple payloads where the first payload that is released at the target site is a NP that in turn carries the active substance further in to the diseased tissue.

3.1 Common classes of nanoparticles for drug delivery

Typical NP drug carrier systems include polymeric materials, inorganic materials and liposomes.⁶⁰ Size, shape and surface chemistry of the NPs are important components to design their biological properties. The main challenge when designing a carrier for biopharmaceuticals is to formulate the drug load in a proper way. The drug has to be stable when it is attached to the carrier and active when it is released. In the following, a few common classes on NPs are highlighted.

3.1.1 Liposomes

In a liposome both hydrophilic and hydrophobic environments are present which enable loading of drugs with totally different properties. Hydrophilic drugs could be loaded in the closed compartment inside the liposome and hydrophobic drugs in the interior of the lipid bilayer. Liposomes are the most common nanocarrier formulations used in clinic today. Liposomal Doxorubicin, which is used to treat Kaposi's sarcoma, metastatic breast cancer, advanced ovarian cancer, and multiple myeloma, was among the first NP formulations on the market. The advantage of delivering the Doxorubicin in liposomes instead of as a pure drug is evident when looking at the circulation half-life. Free Doxorubicin has a half life of 0.2 h in the circulation system but this time increases to 2.5 and 55 h if the drug is administered in an unpegylated or a pegylated liposome respectively.⁷⁸ Furthermore, by using liposomes as drug carriers an active drug release can be achieved at inflamed or cancerous tissue due to the enhanced activity of the secretory phospholipase A2 (PLA2).⁷⁴

3.1.2 Polymeric nanoparticles

There are many types of NPs based on organic polymers.⁷⁹ Polymeric micelles, polymeric vesicles and dendrimers are some of the main groups. Another commonly used type of polymeric NP is polyelectrolyte complexes (PECs) which are created by mixing oppositely charged polyions, where one is the biopharmaceutical to be administered (Figure 6). PECs form spontaneously when the components are mixed and are mainly held together by strong electrostatic interactions. However, other interaction forces like hydrogen bonding, hydrophobic interactions and van der Waals forces complement the electrostatic interactions in PEC formation.⁸⁰ Physical properties like hydrodynamic diameter, zeta potential, and polydispersity of the PECs are dependent on concentration, ionic strength, pH, and properties of the used polymers. Major advantages of using PECs for drug delivery purposes are that they have a slow rate of degradation, are prepared in water solutions, and do not alter normal cell function.⁸⁰ Polycationic polymers have been widely explored for the use in PEC drug delivery systems since DNA, RNA, and most proteins are negatively charged at physiological conditions. Polymers commonly used in such drug delivery systems include biopolymers *e.g.* alginate⁶⁸ and chitosan^{68, 81-83} but also synthetic polymers *e.g.* poly(dimethylaminoethyl methacrylate)⁸⁴ and poly(amido amine)s (PAAs)⁸⁵. In this work several different PECs have been

studied. These particles have been developed for non-invasive (*e.g.* oral, pulmonary, or nasal) administration of human insulin.

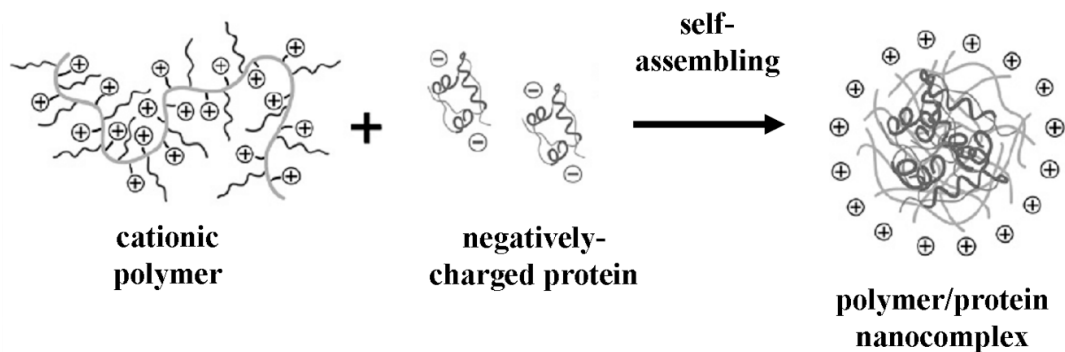


Figure 6. Self-assembly formation of a PEC consisting of a positively charged polymer and a negatively charged protein (Paper II).

3.1.3 Magnetic nanoparticles

Magnetic NPs can be used for many different medical applications. Due to their magnetic properties they can be used as contrast agents for magnetic resonance imaging (MRI) or for magnetic separation purposes, but also to induce hyperthermia or as guidable drug carriers. The particles are most often made of iron oxide, magnetite (Fe_3O_4) or maghemite ($\gamma\text{-Fe}_2\text{O}_3$) and show magnetic properties only when exposed to a magnetic field. When used as drug carriers, magnetic NPs can be concentrated at the target site by a magnetic field. Either a permanent magnet is implanted into the tissue or an external magnetic field is applied. For the magnetic NPs to be attracted by a magnetic field it is important that they are big enough. Too small particles (10-15 nm) are hard to attract towards the blood flow. Other parameters that determine the movement of the NPs are the magnetic field strength and its gradient. Apart from being guided to the diseased tissue, the magnetic NPs can be visualized (diagnostics) and heated by an alternating magnetic field to induce hyperthermia or promote drug release (therapy).^{86,87}

The cell membrane – a biological interface

4.1 Biological barriers and uptake of nanoparticles

A physical barrier that protects the internal environment from the external confines all living entities. For example, the largest human organ, the skin, guards our internal organs, muscles, bones, ligaments, etc., as it constitutes a barrier to the surroundings. Apart from protection, the skin has many other important functions including sensation and heat regulation. Similarly, the cells that our bodies are composed of are confined by a cell membrane. In the following sections the native cell membrane is described in some detail. In addition, the main processes in which NPs may pass this biological barrier and reach the intracellular space are introduced.

4.1.1 The cell membrane

The cell membrane is a fluid, semi permeable barrier surrounding the cell and separating the intracellular space from the extracellular environment. In a cell membrane, lipid molecules are arranged in a two-layered shell (a bilayer) where the hydrophobic parts are facing each other in the interior of the membrane whereas the hydrophilic parts are exposed to the surroundings. See the next section for more information regarding the lipid molecule. The same structure is also found in many intracellular compartments (organelles) where it serves to separate these compartments from the cytoplasm, *e.g.* the cell nucleus, the mitochondria, the golgi apparatus, the endoplasmatic reticulum, the endosome, and the lysosome.

Although the structure of the cell membrane is based on phospholipid molecules it also contains other molecules like proteins, glycoproteins, cholesterol and glycolipids. The amount of protein associated with a membrane differs between different cell types and organelles, although the typical protein content is about 50 % by mass.⁸⁸ The lipid membrane is often described by the fluid mosaic model which was introduced in the early 1970's where the lipid molecules and the associated proteins are allowed to diffuse freely within the membrane.⁸⁹ Although the fluid mosaic model still holds in many respects, the complexity of the cell membrane is today believed to be much greater.⁹⁰ The cell membrane contains a large number of different lipid molecules that in some areas are heterogeneously distributed within the membrane, *i.e.* the cell membrane contains domains with different lipid compositions. These domains (sometimes referred to as rafts) could possibly be functional since their properties, *e.g.* with respect to lipid packing, are altered compared to the surrounding membrane.⁹¹

Proteins associated to the cell membrane, integral and peripheral, allow the cell membrane to carry out a wide variety of different functions. These include transporting nutrients into the cell and waste products out, pump ions or molecules against concentration gradients to keep a proper pH and osmotic pressure inside the cell, form strong connections between neighboring cells to strengthen tissues and create anchoring points for the cytoskeleton to strengthen the cells. Another very important task is carried out by the membrane bound receptors that mediate signals from the surroundings, by binding signaling molecules (hormones or growth factors), to the cytosol leading to various cellular responses. As the membrane proteins play a key role in the cell by sensing the external environment they are important drug targets and much effort is put into studying this class of proteins. About 50% of the drugs on the market target membrane proteins.⁹² Due to the complexity of the native cell membrane, model systems are commonly used to study its properties.

4.1.2 The lipid molecule

Eukaryotic cells have a tremendously complex lipid repertoire consisting of thousands of different kind of lipids.⁹³ Although specific functions have been assigned to certain lipids, there are likely much more to learn when it comes to lipid molecules. Lipids have three main functions in eukaryotic cells. First, lipids are used to store energy, mainly as triacylglycerol and steryl esters. These reserves (lipid droplets) are also used for membrane biogenesis. Second, lipid molecules are the core component in cell membranes. The most common type of lipid in eukaryotic cell membranes is the glycerophospholipid phosphatidylcholine (PC). It accounts for > 50% of the lipids in such membranes. Last, lipids function as first or second messengers in signaling transduction pathways.⁹⁴

Lipids are amphiphilic molecules meaning that they are polar (hydrophilic) on one side and apolar (hydrophobic) on the other. Due to the hydrophobic effect, entropically driven by water, lipids self-assemble in aqueous solutions into larger structures. Depending on the molecular features of the lipids these structures are either micelles, inverted micelles, liposomes or planar bilayer discs.

In this work, four different types of phospholipids have been used to form model membranes; these are 1-palmitoyl-2-oleyl-*sn*-glycero-3-phosphocholine (POPC), 1-palmitoyl-2-oleyl-*sn*-glycero-3-phospho-L-serine (POPS), 1-palmitoyl-2-oleyl-*sn*-glycero-3-phosphoglycerol (POPG) and 1-palmitoyl-2-oleyl-*sn*-glycero-3-ethylphosphocholine (POEPC) (Figure 7). POPC, POPS and POPG occur naturally in cell membranes, while POEPC is produced synthetically. POPC is a zwitterionic lipid with a net neutral charge. POPS and POPG hold a net negative and while POEPC hold a positive charge. Synthetic cationic lipids, *e.g.* POEPC, with various hydrophobic and hydrophilic regions have been developed for liposomal gene delivery. In lipoplexes, complexes between lipid structures and nucleic acids (*e.g.* DNA), electrostatic interactions play an important part.⁹⁵ Because of this, cationic lipids are needed to attract the polyanionic nucleic acids.

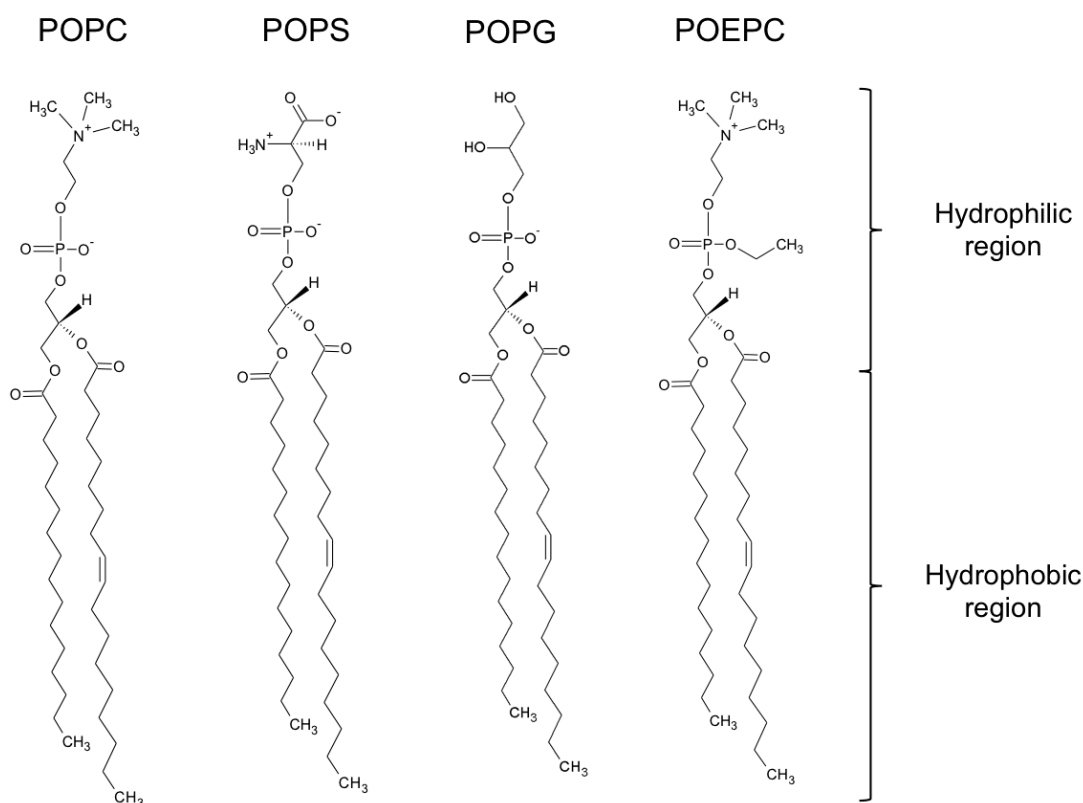


Figure 7. Chemical structures of the four different lipid molecules used in this work.

By selecting these four types of phospholipids it was possible to produce SLBs with different charge. The complexity of the resulting SLBs was of course low compared to native cell membranes, which to a large extent also contain other components.

4.1.3 Cellular uptake of nanoparticles

When studying cellular effect of nanomaterials an important question is if the cells take up these materials. In nanomedicine it is often required, apart from targeting the drug carrying NP to the diseased tissue, that the NP and/or its drug load enters the cell to reach a therapeutic effect. From a risk perspective it is also important to learn where the nanomaterials go upon cellular exposure. The dominating process in which particles are taken up by a cell is called endocytosis.⁹⁶ This process of cellular entry can be divided in three main parts. First, the NP is engulfed by the cell membrane forming membrane invaginations that in turn are released into the interior of the cell forming an endosome. Second, the endosomes are delivered to intracellular structures that enable sorting of the NPs to their final destinations. Last, the NPs are delivered either to various intracellular compartments, back to the extracellular environment, or through the cell (transcytosis). Another way that NPs can pass the epithelial lining, from the apical to the basolateral side, is in between neighboring cells (paracellular transport, Figure 8A). One important physical property of NPs, that is a determinant for the fate of the endosome, is the charge. It has been shown that cationic biodegradable polymeric NPs passed through MDCK epithelial cells (transcytosis) while anionic particles ended up in lysosomes. The route of entry

into the cells was also dependent on the cell type.^{97, 98} Naturally, the size of the nanoparticles is also an important determinant of cellular uptake. It has been shown that spherical gold particles with a diameter of 50 nm induces maximum uptake in HeLa cells.⁹⁹ This result is in line with studies using quantum dots¹⁰⁰ and a recent theoretical study¹⁰¹.

Endocytosis is divided into two subsections called phagocytosis and pinocytosis (Figure 8B). While phagocytosis mainly occurs in specialized phagocytes, *e.g.* macrophages and neutrophils, pinocytosis occurs in all cell types. Different subtypes of pinocytosis are often classified according to the protein involved in the process. This classification gives rise to clathrin dependent and clathrin independent endocytosis. Furthermore, the clathrin independent pathway is divided into caveolae-mediated endocytosis, caveolae and clathrin independent endocytosis and macropinocytosis.

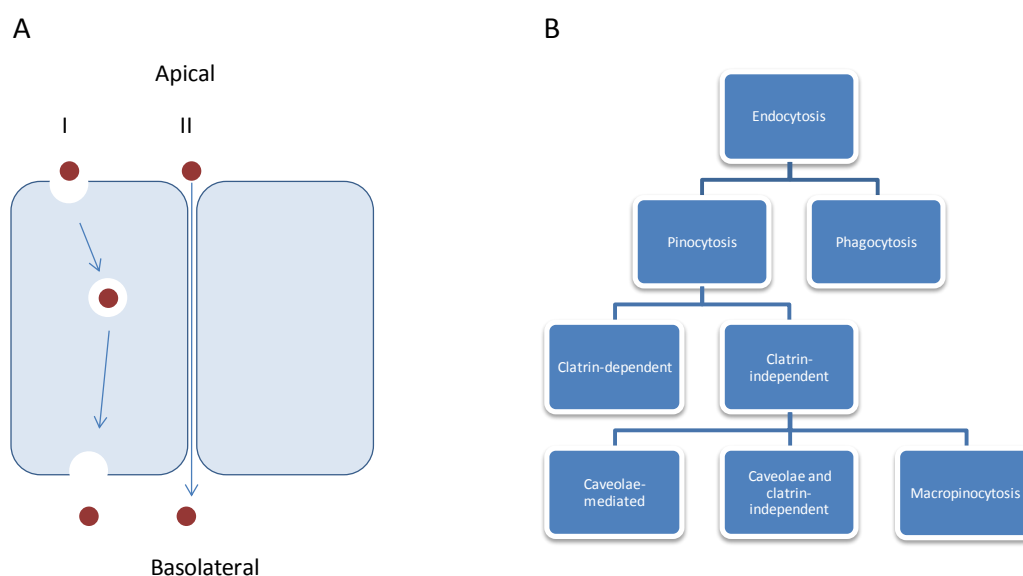


Figure 8. (A) Schematic figure showing the concept of (I) transcytosis and (II) paracellular transport of NPs. (B) Classification of endocytosis.

The two endocytotic pathways that are often considered for uptake of NPs are the clathrin dependent and the Caveolae mediated. Clathrin dependent endocytosis is present in all mammalian cells and responsible for nutrient uptake, *e.g.* iron via the transferrin receptor and cholesterol via the low density lipoprotein receptor. Such natural processes can be utilized for targeting NPs towards endocytosis by decorating them with the appropriate ligands (*e.g.* transferrin) although it cannot be known that the fate of the endosome will be the same if targeted NPs are encapsulated.⁹⁶

Caveolae-mediated endocytosis occurs amongst others in endothelial cells and fibroblasts. Caveolae are a special type of lipid raft rich in cholesterol, sphingolipids and proteins like caveolin-1, cavin and dynamin which all are involved in the endocytosis process. The main feature of caveolae-mediated endocytosis that is of importance to nanomedicine is that it can bypass lysosomes and is prominent for transcytosis. Pathogens such as bacteria and viruses utilize caveolae-mediated endocytosis to avoid degradation.¹⁰² Hence, the same process is believed to be beneficial for delivery of biopharmaceuticals.¹⁰³ One possible target for nanodrugs that has been identified in the caveolae is aminopeptidase P.¹⁰⁴

4.2 Membrane model systems

There is a strong need of better understanding the processes taking place at the cell surface. How does a specific protein interact with its membrane bound receptor? What mechanisms determine the way a foreign nano-sized particle interacts with a cell membrane? Questions like these are hard to assess when working with living cells due to the complexity of the system. By using a model system, the degree of complexity could be decreased tremendously and the interaction processes could be studied by a wide variety of analytical techniques, which are not applicable to entire cells. Following this methodology a more fundamental understanding of the interaction processes is gained. Common membrane model systems include liposomes, supported lipid bilayers, and Langmuir-Blodgett films (Figure 9).

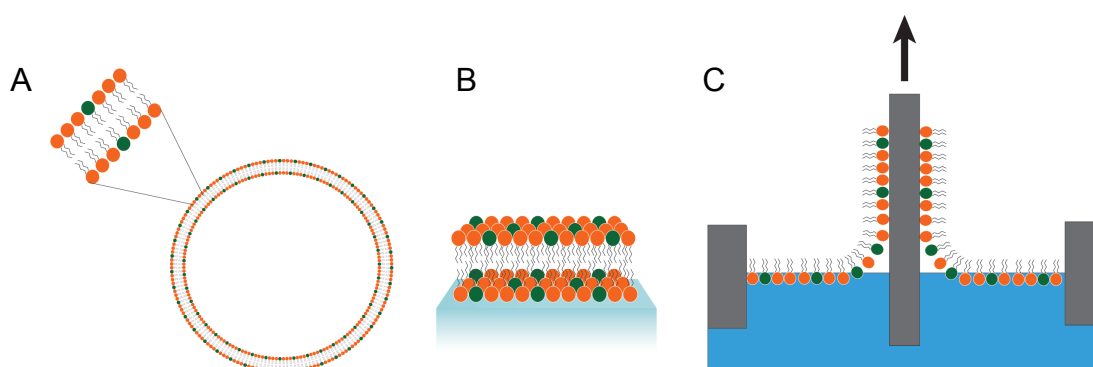


Figure 9. Schematic images of common membrane model systems. (A) liposome, (B) supported lipid bilayer and (C) Langmuir-Blodgett deposition.

4.2.1 Liposomes

Liposomes are spherical entities that consist of a lipid bilayer shell enclosing an aqueous interior.¹⁰⁵ It is possible to produce liposomes in a wide range of sizes, from diameters of a few tenths of nanometers to several hundred micrometers. Often liposomes are referred to as lipid vesicles and classified according to their size and lamellarity. This classification yields small (SUV), large (LUV) and giant (GUV) unilamellar vesicles. Although several different techniques can be used to produce unilamellar vesicles, extrusion is the most common. In this technique, which was first introduced by Hope *et al.* in 1985¹⁰⁶, a lipid suspension is pressed back and forth through a polycarbonate membrane with a well-defined pore size. Later, in 1991, a convenient device for extruding liposomes in volumes up to 1 mL was described and evaluated.¹⁰⁷ By changing the pore size of the membrane the final size of the liposomes can be tuned. The main advantage of using liposomes instead of supported lipid bilayers is that an aqueous environment is present on both sides of the lipid bilayer. Due to this it is possible to incorporate large transmembrane proteins in their native conformation into the lipid bilayer shell of the liposomes. However, it is difficult to probe the interior compartment of the liposome, which would be necessary for measuring for example charge translocations across the membrane.

4.2.2 Supported lipid bilayers

In this work, supported lipid bilayers (SLBs) were used as a model system for the native cell membrane and are here described in more detail. An SLB is formed on a solid support (sensor surface), typically coated with SiO_2 , by adsorption and rupture of liposomes leading to the formation of an extended planar bilayer. The rupture of the adsorbed liposomes is for most lipid compositions initiated at a certain surface coverage due to mechanical strain between adjacent liposomes. The initial rupture of liposomes form patches of bilayers that in turn fuse and form a continuous SLB.^{19, 108, 109} SLBs could be formed over large areas (in the order of cm^2) and are fluid in their nature. The simplest SLB consist of only one type of lipids. From this starting point the complexity could be increased by changing the lipid composition or the membrane morphology. The latter typically occur when an amphiphile is added to the membrane.¹¹⁰ Since the SLB is placed directly on the support, only separated by a thin layer of water molecules, the incorporation of transmembrane proteins is difficult. These proteins will lose their mobility in the lipid membrane and their function due to the close proximity to the solid support. To solve this problem the SLB could be formed on a polymer cushion or a tether can be placed between the surface and the membrane.¹¹¹⁻¹¹³ Since the SLB is confined to a solid support a variety of surface sensitive techniques can be used for the analyses, *e.g.* AFM, QCM-D and reflectometry.^{114, 115} In Figure 10 a schematic of a SLB on a QCM-D sensor surface is shown.

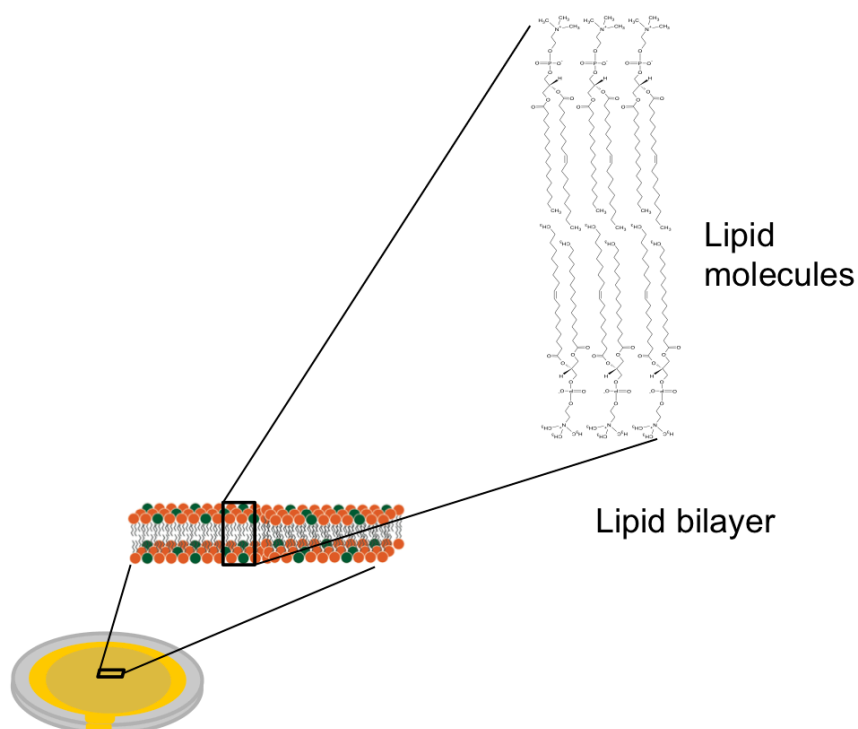


Figure 10. Schematic model of a supported lipid bilayer formed on a QCM-D sensor surface.

4.2.3 Langmuir-Blodgett films

Another commonly used model system of the cell membrane is Langmuir-Blodgett (LB) films¹¹⁶. The LB technique, in which the model membrane is formed, can be divided in two main parts. First, an organized layer of amphiphilic molecules (*e.g.* lipids) is formed at an air-water interface (Langmuir monolayer) and second, a substrate is vertically passed through the interface transferring the Langmuir monolayer to the substrate. The substrate can be passed through the monolayer repeatedly, and for each pass an additional monolayer of the amphiphilic molecules is added. In this way it is possible to build multilayered assemblies on the substrate. The Langmuir monolayer, which by itself can be used as model system for the cell surface, is formed inside a trough in which the surface area can be altered. This makes it possible to alter the local density and organization of the molecules by regulating the lateral pressure. At a surface pressure of 30 mN/m the lipid packing density is similar to a cell membrane.¹¹⁷ At this point, drugs or drug loaded NPs can be added to the subphase and the change in surface pressure can be studied.¹⁵ Naturally, Langmuir monolayers cannot be used as a model to study transport processes across a cell membrane since it only consists of one lipid layer and is located at an air-water interface. Despite this, this type of model system can be used to mimic the outer surface of a cell. Other advantages with using lipid monolayers as a model system, apart from the possibility to control the surface pressure, are that the lipid composition, temperature and subphase content are controlled.¹¹⁸

As mentioned, it is possible to form a bilayer on a solid support from the Langmuir monolayer by the LB technique. This is performed by first forming a lipid monolayer on the surface of the subphase and then transferring the substrate first downwards and then upwards through the interphase. The same result can also be obtained by a combination of the LB and the Langmuir-Schaeffer (LS) techniques. In the LS technique¹¹⁹, a Langmuir monolayer is formed and subsequently a hydrophobic substrate is placed horizontal to the subphase and kept in contact with the Langmuir monolayer for 30-60 s. In this way the Langmuir monolayer is transferred to the hydrophobic substrate. To form a lipid bilayer with a combination of the two techniques, the first layer is transferred by the LB technique and the second by the LS technique.

4.3 Forces at the nano-bio interface

When considering the forces that may be exerted between nanomaterials and a cell membrane it is easy to realize that a vast number of interactions are possible. As a starting point, it may be useful to consider the interactions between colloidal particles in suspension, including *e.g.* steric, electrostatic, solvent, and Van der Waals interactions (Figure 11A).¹²⁰

To obtain a stable NP suspension, the NPs are commonly stabilized by steric or electrostatic means. Steric stabilization is obtained by functionalizing the surface of the nanoparticle with a polymer, *e.g.* PEG. When two polymer-coated surfaces approach each other they experience a repulsive force due to the unfavorable entropy associated with the confinement of the polymers (upon compression). In nanomedicine, the same strategy is used to avoid plasma protein adsorption on the surfaces of drug carriers, resulting in a decreased

cellular uptake.¹²¹ Electrostatic stabilization of the NP suspension is achieved for NPs possessing a sufficiently high surface charge. Charged NPs of the same type will be kept away from each other due to electrostatic repulsion. In suspension, the surface charges are balanced by counter ions in the solution. These ions form an electrical double-layer surrounding the NPs. More specifically, the electrical double-layer consists of tightly bound ions close to the surface (Stern layer) and more loosely bound ions further away from the surface (diffuse layer). Generally, electrostatic interactions can occur over a long range (hundreds of nanometers) compared to other types of interaction forces. However, at a high ionic strength, *e.g.* in a biological medium, this force is efficiently screened some nanometers from the surface.

In addition to steric and electrostatic interactions, solvation is another important phenomenon for the stability of NPs. For lyophilic materials, *i.e.* materials that have an affinity for the surrounding dispersion medium, the solvent molecules bind strongly to the surface of the nanoparticles and form a protective layer that prevent particle aggregation. This effect is referred to as solvation. If the dispersion medium is water, the same effect is commonly called the hydration force. Another important interaction between NPs is the Van der Waals force. This force originates from quantum mechanical fluctuations of electrons in the material. These fluctuations produce a dipole in the particle that in turn induce a dipole in an adjacent particle. The Van der Waals force between similar materials are always attractive.¹²² The interactions between colloids, or colloids and surfaces, are described by the well-established DLVO-theory (after Derjaguin, Landau, Verway, and Overbeek). This theory combines the repulsive electrostatic interactions and the attractive Van der Waals forces and makes it possible to calculate a distance dependent interaction potential between the interacting entities (Figure 11B).

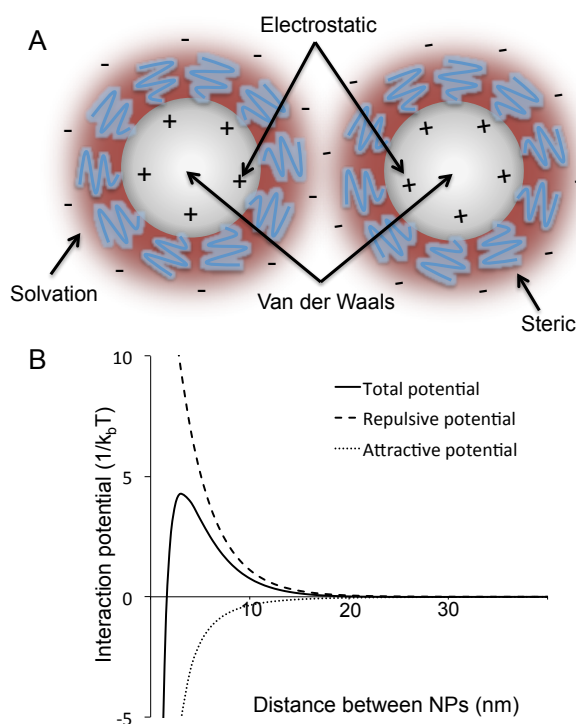


Figure 11. (A) The major interaction forces between two NPs in suspension. (B) Example of a distance dependent interaction potential between two NPs according to DLVO-theory. The solid line is the sum of attractive Van der Waals forces and repulsive electrostatic interactions.

The studies presented in Paper I-IV regard the interactions between nanomaterials and SLBs. Although the mentioned forces still apply, the situation is somewhat different in such systems compared to the interactions between colloids. Now, two different entities (NP and SLB), with fundamentally different properties (shape, size, composition etc.) interact (Figure 12). In the studies, the composition of the supported lipid bilayer was varied, *i.e.* the electrostatic interactions between the NP and SLB were tuned to be either repulsive or attractive. In addition, the fluid nature of the lipid membrane allows for segregation of different types of lipid molecules upon NP interactions. It is also important to be aware of the fact that the lipid membrane is supported on a solid substrate, which may have an impact on the studied interactions, due to *e.g.* restricted flexibility of the membrane or induced asymmetry between the two leaflets.

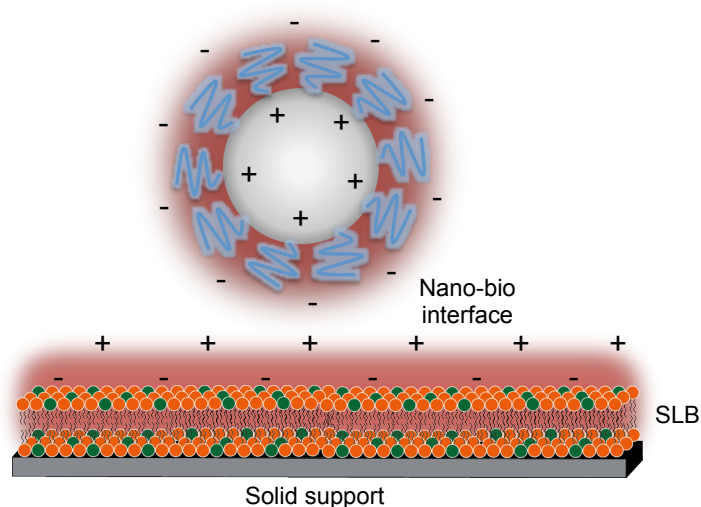


Figure 12. Schematic representation of the interface between a positively charged NP and an oppositely charged SLB. The electrical double-layers at their surfaces are represented by counter charges.

If we now consider the interaction between a NP and the cell membrane on a living cell, the complexity of possible interactions increases even further.¹²³ As described in section 4.1.1, the cell membrane contains many components apart from the core structure of lipid molecules. For this reason, specific interactions between NPs and biomolecules contained in the cell membrane are possible. Interaction between specific membrane bound receptors and ligands presented at the NP surface is commonly utilized for targeting nanodrugs to their intended site of action. Membrane bound proteins may also alter the extracellular environment, *e.g.* through active transport of proteins and ions across the cell membrane, and affect the interaction forces. In addition, the cell membrane is a non-rigid structure that could deform upon NP interaction, yielding an increased contact area. This process may result in uptake of the NP through endocytosis, a process that is further described in section 4.1.3. Furthermore, the surface of the cell membrane is not homogenous. For example, a heterogeneous charge distribution over the surface gives different interaction potentials depending on where the interactions take place. Naturally, for particles much larger than the length scale of the heterogeneities this effect is averaged out.

Another parameter that is important to consider upon NP-cell membrane interactions is the possible transformations of the NP when dispersed in a biological medium.^{124, 125} When entering a biological medium, the surface of the NP will become coated with proteins, forming a protein corona. This process shapes the surface properties and alters the hydrodynamic size of the NP. Since the protein corona largely determines the cellular interactions it is of high interest to learn how the protein corona depends on the particle composition.^{126, 127}

4.4 From membrane models towards whole cell analyses

Although membrane model systems are commonly used as cell membrane mimics, it is not straightforward to predict the outcome of *in vitro* cell assays based on model membrane experiments. However, I do not believe that such comparisons should be made, at least not until proper structure activity relationships have been established. Instead, the two types of analyses should be used as complement to each other, similar to the way that cell testing relates to animal studies. When it comes to studies of NPs using cell cultures, the endpoints often relate to NP induced cytotoxicity or to the fate of the NPs, *e.g.*, uptake and intracellular localization.

There exist a wide variety of cytotoxicity assays, but the majority relates cell death to a colorimetric output. In turn, these methods are based on either the integrity of the plasma membrane or the mitochondrial activity.¹²⁸ If the integrity of the plasma membrane is compromised upon NP exposure, there will be leakage of intracellular contents that are detected in the cytotoxicity assays. For example, released amount of lactate dehydrogenase (LDH) is proportional to the number of damaged or lysed cells.¹²⁹ It is also possible to determine if a cell is alive or dead by testing the mitochondrial activity.¹³⁰ One such test that is commonly used is the MTT viability test. Furthermore, the levels of glutathione can be analyzed to detect oxidative stress, *e.g.*, lipid peroxidation, as a sub-lethal cellular response to nanoparticle exposure. Such exposure may also cause inflammation, which could be tested by analyzing the levels of pro-inflammatory cytokines and proteins, *e.g.*, IL-1 β , IL-6, and TNF- α .

The use of surface sensitive analytical techniques to monitor cellular responses caused by external stimuli, such as NP exposure, is not yet widely acknowledged. However, when it comes to acoustic sensors their use in cell studies is increasing. See section 5.2.1 for further information regarding QCM-D and cells. Surface acoustic techniques may be used to probe cell-surface interactions and the mechanical properties of the cell. In both these areas the cytoskeleton play a vital role.

The cytoskeleton of eukaryotic cells is composed of three main fibrous structures: actin filaments (7-9 nm in diameter), microtubules (24 nm in diameter), and intermediate filaments (10 nm in diameter). These structures are responsible for supporting the cell membrane and form the shape of the cell. Unlike the skeleton of vertebrates, the cytoskeleton undergoes constant rearrangements that may generate movements of the cell. Another essential function of primarily the actin filaments and the microtubules is that they form tracks along which organelles can move in the cytosol. Motor proteins such as myosin V, kinesin, and dynein mediate this transport. One example of rapid,

synchronous, and bi-directional transport of organelles in the cytosol is the transport of pigment granules (melanosomes) in melanophores.¹³¹ Melanophores, which are present in the skin of many fish, amphibians, and reptiles, are involved in the color change of the animals in response to external stimuli. Depending on the intracellular distribution of melanosomes the cells appear dark (dispersed state) or bright (aggregated state). The transport of melanosomes can be triggered either by melanocyte stimulating hormone (MSH) or melatonin, which induce dispersion and aggregation respectively (Figure 13).¹³²

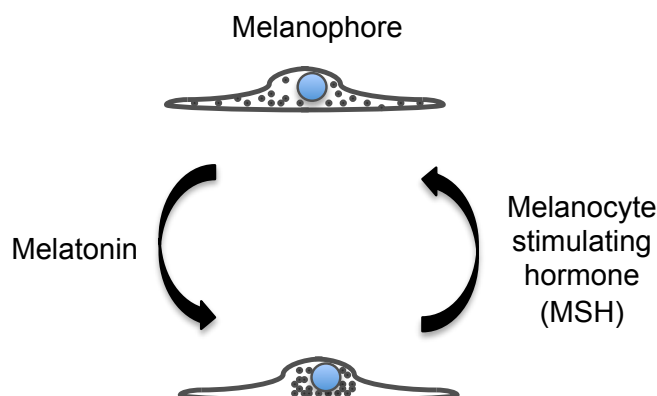


Figure 13. Schematic figure of the melanosome distribution a melanophore. Melatonin induces aggregation of melanosomes close to the cell nucleus while MSH induces dispersion of the melanosomes throughout the cell.

Due to their large size and light absorbing properties melanosomes are easily visualized by ordinary optical microscopy. For this reason, together with the fact that redistribution of melanosomes is easily induced, melanophores are often used as a model system for studies of intracellular transport, *e.g.* of molecular motors¹³³⁻¹³⁵ or the cytoskeleton¹³⁶.

Taken together, melanophores provide a good model cell line to be used in QCM-D studies. Such studies will push the development and use of this technique in cell studies in general. In paper V, the intracellular transport of melanosomes is monitored by QCM-D, a methodology that subsequently was applied to study effects of NP exposure on this process.

Experimental techniques

This chapter gives a brief introduction to the analytical techniques used in this work. Apart from the first technique (dynamic light scattering), that was applied to characterize nanoparticles in bulk, all techniques are surface based. The main technique throughout this work has been the quartz crystal microbalance with dissipation monitoring (QCM-D). This technique has been complemented with other surface sensitive techniques, *e.g.*, AFM, DPI, or reflectometry, depending on the system under study. The specific application where QCM-D is used to study cells is highlighted in section 5.2.1.

5.1 Nanoparticle size and zeta potential measurements

Dynamic Light Scattering (DLS), also known as Photon Correlation Spectroscopy (PCS), is a technique that is used to determine the size of colloidal particles or macromolecules in solution.¹³⁷ The technique takes advantage of the Brownian motion of particles in solution. Brownian motion is a stochastic process due to collisions with surrounding molecules. When illuminating the suspension with laser light, the light will be scattered by the particles and due to the Brownian motion the intensity of the scattered light will fluctuate over time. The time-dependant fluctuation is measured and used to determine an autocorrelation function. In autocorrelation measurements the signal is constantly compared to itself using a small time shift, τ . The correlation of the signal, G , decays exponentially and the rate is determined by the diffusion of the particles.

$$G = \int_0^{\infty} I(t)I(t + \tau)dt = B + Ae^{-2q^2D\tau} \quad (1)$$

In equation 1, B is the baseline, A the amplitude, q the scattering vector and D the translational diffusion coefficient. The scattering vector is calculated according to equation 2 where n is the refractive index of the solvent, λ_0 is the wavelength of the laser in vacuum and θ is the scattering angle.

$$q = \frac{4\pi n}{\lambda_0} \sin\left(\frac{\theta}{2}\right) \quad (2)$$

By measuring the speed of the Brownian motion, the translational diffusion coefficient, D , is obtained (eq 1). Using the Stokes-Einstein equation (eq. 3), this diffusion coefficient can be used to calculate the hydrodynamic diameter, D_H .

$$D_H = \frac{kT}{3\pi\eta D} \quad (3)$$

In equation 3, k is the Boltzmann constant, T is the temperature and η is the viscosity of the dispersant.

If the sample consists of several size populations it is possible to determine their individual sizes by using distribution algorithms.¹³⁸ However, the result depends on several factors such as the relative sizes of the different populations and their relative scattering intensity as well as their polydispersity. The result is

given as an intensity distribution where the percentage of the intensity of the scattered light is shown as a function of the particle size. This data could be recalculated to a number distribution. Since the scattering intensity is related to the particle diameter by a factor of 10^6 , the presence of large particles will dramatically influence the intensity distribution while small particles will have a much smaller effect.

By electrophoretic light scattering it is possible to determine the zeta potential of nanoparticles. Around a charged particle there exist layers of counter ions, *i.e.* ions of opposite charge. In the inner layer, the ions are tightly associated with the particle (Stern layer) and in the outer layer the ions are more diffusely associated. Inside the diffuse layer there is a boundary called the slipping plane. Within the slipping plane the ions move together with the particle as a stable entity in an electric field. The potential at the slipping plane is commonly referred to as the zeta potential or mean surface charge. To determine the zeta potential, an electric field is applied across a suspension of the particles. When equilibrium between the electric and the opposing frictional forces is reached, the particles are travelling at a constant velocity (electrophoretic mobility, U_E). This velocity is measured by laser doppler velocimetry. The electrophoretic mobility could then be used to calculate the zeta potential by using the Henry equation (eq. 4)

$$U_E = \frac{2\varepsilon z f(ka)}{3\eta} \quad (4)$$

In equation 4, ε is the dielectric constant, z is the zeta potential, $f(ka)$ is Henry's function and η is the viscosity. When measurements are performed in aqueous media at moderate electrolyte concentrations, Henry's function can be estimated to 1.5 according to the Smoluchowski approximation.

5.2 QCM-D

Quartz crystal microbalance with dissipation monitoring (QCM-D) is a technique that measures small mass changes on a sensor surface, and the viscoelastic properties of the attached material. The experimental setup and a quartz sensor are shown in Figure 14. QCM-D is a well established surface sensitive technique which has been used to study the formation of SLBs^{108, 139} and their biomolecular interactions¹⁴⁰. The sensitivity of the technique is very high and masses in the order of ng/cm^2 can be detected. The technique is built upon a piezoelectric quartz crystal. This means that when the crystal is subjected to mechanical stress electric charges are generated on its surface, and when an electric field is applied the crystal is strained. In most QCM-D setups, AT-cut quartz crystals are used and the surfaces of the disc shaped sensors are covered with thin metal electrodes. An AT-cut crystal is cut in an angle of 35.25° from its optical axis and oscillates in thickness shear mode when subjected to an oscillating electric field. Resonance occurs when the frequency of the applied field corresponds to the fundamental frequency of the crystal or to an overtone thereof.¹⁴¹

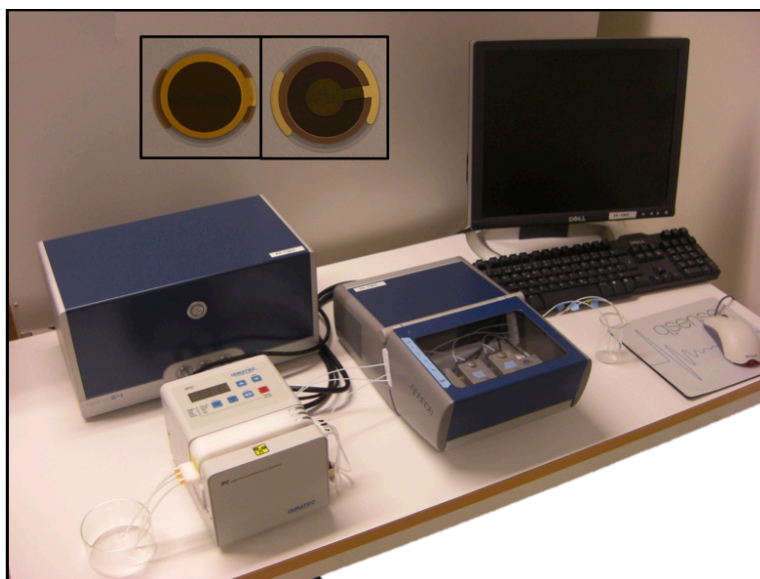


Figure 14. Photo of a QCM-D E4 setup (Q-Sense). The inset shows the two faces of a QCM-D sensor. To the left is the upper surface (sensing surface) and to the right is the lower surface that connects the top and bottom electrodes to the instrument.

Mass associated to the sensor surface induces a decrease in the resonance frequency (Figure 15). If the mass ($m_{acoustic}$) is small compared to the mass of the crystal, evenly distributed in a thin layer, rigidly coupled and does not slip, it is proportional to the induced shift in frequency (Δf_z). This relationship is described by the Sauerbrey relation (eq. 5).¹⁴²

$$m_{acoustic} = C \cdot \frac{\Delta f_z}{z} \quad (5)$$

C, the mass sensitivity constant, is $-17.7 \text{ ng}/(\text{cm}^2 \text{ Hz})$ for an AT cut crystal with a fundamental frequency of 5 MHz and z (1, 3, 5, 7, 9, 11 or 13) is the number of the harmonic.

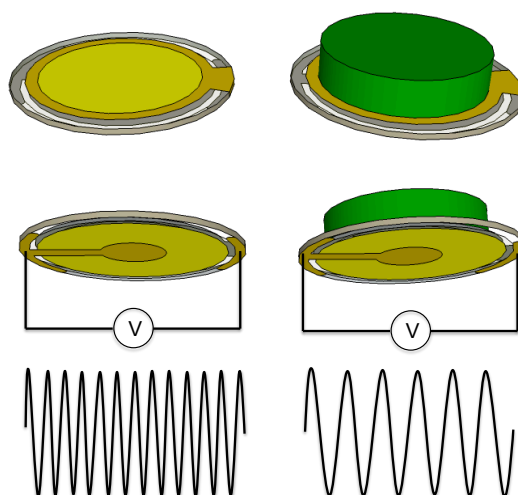


Figure 15. The principle of QCM sensing. By applying an alternating voltage across the sensor induces oscillations of the quartz at its resonance frequency (left figure). When mass is associated with the sensor surface the resonance frequency decreases (right figure).

In non rigid films, shear acoustic waves propagates differently than in the quartz crystal. Due to this, the crystal and the attached film cannot be considered as one unit and the Sauerbrey equation is no longer valid. Apart from the frequency, the dissipation factor (D) is also measured in the QCM-D technique. This factor derives from decay rate of the voltage over the crystal when the driving voltage is turned off and is described by the following relation (eq. 6).¹⁴³

$$D = \frac{E_{dissipated}}{2\pi \cdot E_{stored}} \quad (6)$$

$E_{dissipated}$ is the energy dissipated during one period of oscillation and E_{stored} is the energy stored in the oscillating system. The dissipation factor correlates to the viscoelastic properties of the attached material, very rigid films have low dissipation and loosely attached materials generate high dissipation (Figure 16).

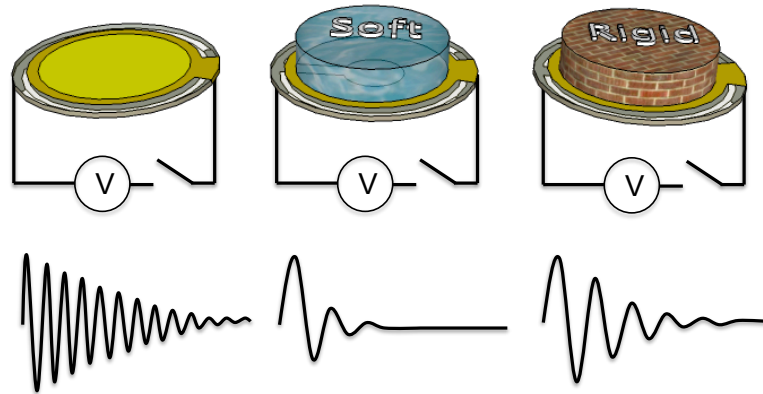


Figure 16. The principle of the dissipation response. When the driving voltage is switched off the oscillations of the sensor is damped as energy is dissipated. The oscillation amplitude decreases slowly in the case of a bare sensor surface (left figure). If a soft material is associated with the sensor surface the damping occurs rapidly (center figure). In a more rigid system the damping occurs more slowly (right figure).

The oscillatory motion of the quartz crystal generates a decaying wave that extends away from the sensor surface. How long the wave extends, *i.e.*, the penetration depth (δ) is determined according to Equation 7.¹⁴⁴

$$\delta = \sqrt{\frac{2\eta}{\omega\rho}} \quad (7)$$

where η is the shear viscosity and ρ the density of the medium. The penetration depth also depends on ω , the angular frequency of the quartz crystal. Note that δ is proportional to $\sqrt{\eta}$ and to $1/\sqrt{f}$ (since $\omega = 2\pi f$), where f is the resonance frequency for a specific harmonic (*e.g.* 5 MHz). At room temperature the penetration depth of a 5 MHz sensor in water is about 250 nm for the fundamental frequency ($z = 1$) and about 150 nm for the third harmonic ($z = 3$).

In QCM-D instruments all mass associated with the sensor surface are measured, not only the “dry” mass. This property is evident when studying the formation of SLBs by liposome rupture. First, intact liposomes adsorb to the sensor surface generating large shifts in both frequency and dissipation. The large responses are due to the floppy structure on the surface and the large amount of liquid associated with the intact liposomes, both in their interior and

between adjacent liposomes. Second, the liposomes start to rupture and release the enclosed liquid to the surroundings, a process that lead to a decrease in the frequency and dissipation shifts. Finally, when the SLB have been formed, the frequency and dissipation shifts reach characteristic values of -26 Hz and < 0.5 respectively.

5.2.1 QCM-D and cells

Although QCM-D is commonly applied in studies of thin layers, normally composed of a low number of components, the technique is also used in studies of cells. Within the last decade, QCM-D (and QCM) has become a well established technique in this area of research and serve as a good complement to traditional microscopy analyses.^{145, 146} One advantage with this technique compared to microscopy is that it averages the responses from a population of cells and is not subject to the variability present in single cells analyses. Other main advantages with QCM-D are that it measures in real time and is non-invasive. However, one putative effect that could potentially affect the cells' ability to grow on the sensor is the shear oscillations of the surface. This effect has been examined and it was shown that the adhesion kinetics and the formation of focal adhesion points were only affected at oscillations amplitudes exceeding 20 nm.¹⁴⁷ Typically, the lateral oscillation amplitude is in the order of 1 nm, hence the technique could be claimed to be non-invasive.

The main research areas where QCM is applied in cell studies include cell adhesion, spreading, and proliferation. In such studies, the surface properties are very important. Often, in the QCM experiment, the substrate is coated with serum proteins (either *ex situ* or *in situ*) to promote cell adhesion in a similar way as in conventional cell cultures. To study cell adhesion in further detail, the technique may be used to evaluate functionalized sensor surfaces. For example, surface coatings presenting the RGD peptide have also been used to control the adhesion of cells.¹⁴⁸ Furthermore, studies of cellular responses to soluble agents, *e.g.* drugs and fixation reagents, also suit the QCM-D technique. It has been demonstrated that alterations in the cytoskeleton, caused by *e.g.* cytochalasin D^{149, 150} or nocodazole¹⁵¹, are detected by QCM(-D). In particular, one trend that has been noted is that the cortical actin cytoskeleton is a major contributor to the cellular acoustic response.¹⁵² The cellular responses are also predominantly attributed to changes close to the sensor surface, *i.e.* to the cell substrate interface. Naturally, due to the limited penetration depth of the sensor, changes occurring close to the sensor surface are likely to generate acoustic responses. It should be noted, however, that the cause of the observed responses not necessarily needs to be localized close to the substrate, it could be an indirect effect (within the penetration depth) that is sensed. For example, in a study by Cans *et al.* exocytosis and retrieval of exocytosed vesicles from the upper membrane generated responses in both Δf and ΔD .¹⁵³ In that study it was speculated that the variation in membrane area, and the resulting change in the lateral tension of the membrane, generated the observed responses. An alternative explanation of the observed responses could be based on the possible tensegrity of the cytoskeleton. Tensegrity is one model of the mechanical properties of the cytoskeleton, stating that the cell stiffness is roughly proportional to the intracellular stress.¹⁵⁴ In the process of exocytosis (and

endocytosis) the cytoskeleton will be affected and remodeled, and despite that the processes occur at the apical cell membrane the intracellular strain (tensegrity) will enable acoustic detection close to the substrate. The concept of tensegrity was first described by the architect R. Buckminster Fuller in 1961¹⁵⁵ and is nicely visualized by the artist K. Snelson.

In line with the aim of the work presented in this thesis, QCM has recently been applied to study cytotoxic effects of nanomaterials, specifically macrophages were exposed to single walled carbon nanotubes.¹⁵⁶ Additionally, in the same study, phagocytosis of nanoparticles (non-toxic polystyrene beads) was probed for the first time using QCM.

5.3 AFM

Atomic force microscopy (AFM) belongs to a family of scanning probe microscopy techniques that stems from the scanning tunneling microscopy (STM) technique developed in the early 1980's. The invention of the AFM in 1986 made it possible to analyze all surfaces, not only the ones that are electrically conductive as is the case for STM. This advantage, together with the possibility to perform analyses in liquid environments, opened up the door to the field of biology. From now on it was possible to resolve features on biological samples much smaller than the optical diffraction limit.¹⁵⁷

The four main components in a typical instrument are the cantilever to which a sharp tip is attached, an optical system used to detect cantilever deflection, the piezoelectric translation system, and the feedback circuitry (Figure 17). The cantilever is usually fabricated from silicon or silicon nitride and has a spring constant between 0.01 and 100 N/m. The piezoelectric translation system typically consists of a tube made from a piezoelectric ceramic. This system raster scans the tip over the sample, where the movements can be controlled with high accuracy in three dimensions. The optical deflection system measures the bending of the cantilever that in turn is dependent on the tip-sample interaction (*i.e.* "force").

An AFM analysis can be performed either in contact or in tapping mode. In contact mode the tip will be in constant contact with the surface, and the image is created from either the bending of the cantilever or the movements of the cantilever base in the z-direction. These two ways of detection are called constant height and constant force, respectively. In the latter case the data from the optical deflection system is fed into a feedback loop, which keeps the deflection of the cantilever (*i.e.* the force) constant. In tapping mode the cantilever is made to oscillate close to its natural resonance frequency. When the tip comes in close contact with the surface, the oscillation amplitude will change due to tip-sample interaction. When the tip is scanned across a surface, the amplitude is kept constant by the feedback loop, and the necessary scanner height adjustments are used to form an image. In this work, only contact mode AFM at constant force has been applied.

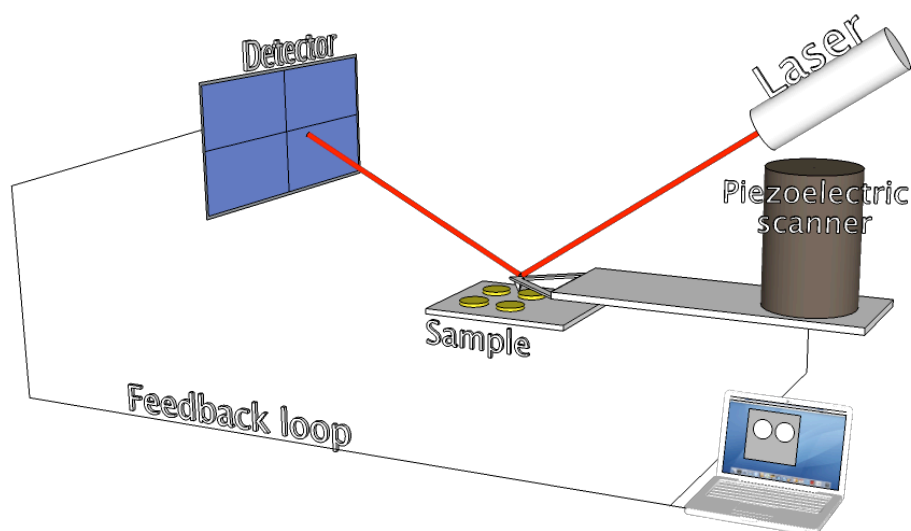


Figure 17. Schematic illustration of an AFM setup.

The AFM can also be used for force spectroscopy, *i.e.* the force is measured versus the distance between the tip and the sample at a fixed lateral position. With force spectroscopy, intermolecular forces can be measured and the force spectra can indicate the length or thickness of an investigated object.¹⁵⁸ This is a good way to detect the presence of a SLB on a surface. Since the membrane is very flat and faithfully follows the contours of the underlying substrate, a topographic image will not easily reveal its presence. The outcome of the force spectra will however be different if a membrane is present compared to the bare surface.

5.4 DPI

Dual polarization interferometry (DPI) is a surface sensitive analytical technique developed in the early 2000s.¹⁵⁹ The technique is based on a dual slab waveguide and similarly to other analytical techniques, *e.g.* SPR and TIRF, it relies on an evanescent field that extends 100-200 nm from the sensor surface into the liquid compartment. The DPI waveguide consists of an upper sensing waveguide and a lower reference waveguide where the top surface of the sensing waveguide is the actual sensor surface. The principle of the DPI setup is illustrated in Figure 18. Polarized laser light ($\lambda = 623.8$ nm) is applied at one end of the waveguides, and as the light propagates along the sensing waveguide the phase of the light changes in relation to the adsorption events that take place on the sensor surface. In the lower waveguide, the light is not influenced by the adsorption events. When the light reaches the far end of the waveguides, it diverges and is allowed to combine. In this way interference fringes, light and dark bands, are formed and can be detected on a screen positioned beyond the waveguides. The position of the interference fringes depends on the phase relationship of the light from the two waveguides. In this way it is possible to relate the adsorption events with a measurable output. Two orthogonal polarizations of the incident light, transverse magnetic (TM) and transverse electric (TE), are used. These two polarizations generate independent measurements that respond differently to binding events on the sensor surface.

From the two measurements, the density and the thickness of the adsorbed material can be extracted using classical optical theory.

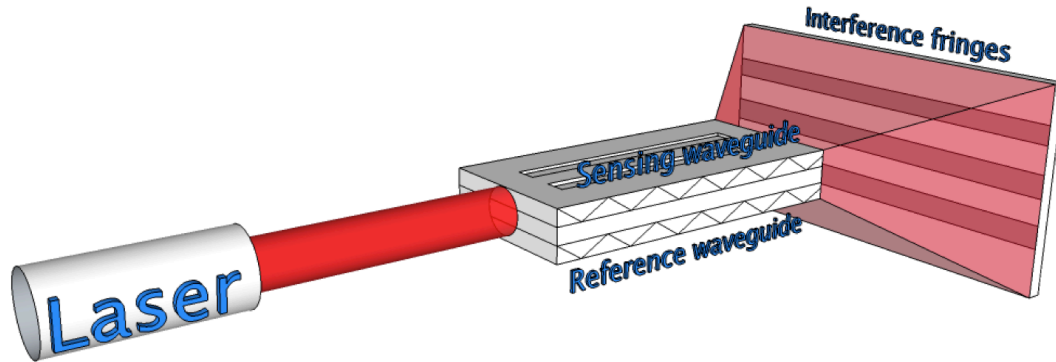


Figure 18. Schematic of the DPI setup. Laser light is introduced into two parallel waveguides in the sensor chip and interference fringes are formed in the far end. The position of these fringes is dependent on the phase shift of the light traveling in the sensing waveguide, which in turn depend on the mass deposition on the sensor surface. The polarizer is omitted from the figure for increased clarity.

Until now, DPI has been applied in many different fields of research, *e.g.*, protein adsorption¹⁶⁰ and lipid membrane formation^{161, 162}. With DPI it is also possible to address the anisotropic properties of the adsorbed material. As opposed to isotropic materials, the properties of anisotropic materials depend on the direction. For example, the refractive index of a material, or molecule, in the x and y dimensions (n_x and n_y) may differ from the refractive index in z (n_z). In DPI analyses it is possible to study the anisotropic properties of lipids in a supported membrane. In this case, the lipid molecules are ordered perpendicular to the sensor surface, a structure that generates a positive birefringence in the DPI data analysis. Birefringence is the difference between the extraordinary (n_e) and the ordinary (n_o) refractive index of the material on the surface. This difference corresponds well to the difference in refractive index determined using the TM and TE polarizations of the incident light ($n_{TM}-n_{TE}$). In Figure 19 the difference between anisotropy and birefringence is shown.

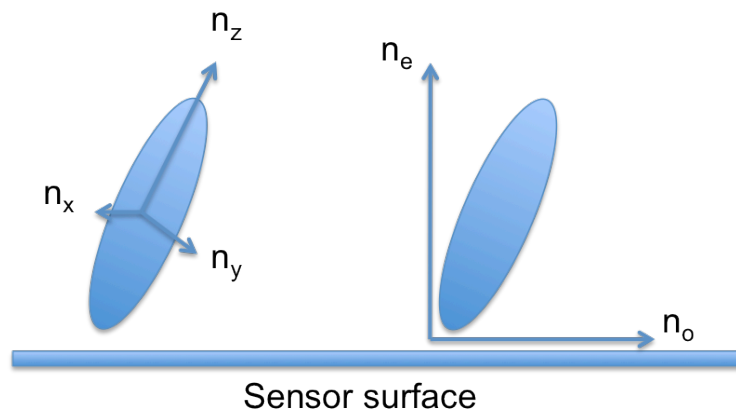


Figure 19. The refractive index of anisotropic materials is directionally dependent, *i.e.*, n_x and n_y differ from n_z . The difference between the extraordinary refractive index (n_e) ($n_e \approx n_{TM}$) and the ordinary refractive index (n_o) ($n_o \approx n_{TE}$) is termed birefringence and is determined in the DPI data evaluation.

5.5 Reflectometry

In contrast to QCM-D, reflectometry is an optical technique. This difference in sensing principle makes the two techniques an excellent complement to one and other. While QCM-D senses the hydrated mass ($m_{acoustic}$) associated to the sensor surface, optical techniques only detects the “dry” mass (m_{optic}). When combining the two techniques the degree of hydration of the adsorbed material could be determined.¹¹⁵ Reflectometry is based on the fact that the optical property, the reflectivity, of a surface changes when mass is adsorbed to it. The surface under study is illuminated through a prism with monochromatic, plane polarized light at a certain angle of incidence. The reflected light is split in two components with different polarizations and the intensity ratio (S) of these two polarizations is monitored. This ratio changes when adsorption/desorption processes occurs at the surface and the relative changes is given as the output ΔR .

$$\Delta R = \frac{S-S_0}{S_0} \quad (8)$$

S_0 corresponds to the initial intensity ratio, *i.e.* only buffer. The optical output, ΔR , is related to the adsorbed mass through the following equations

$$\Delta R = d \cdot (n - n_0) \cdot A \quad (9)$$

$$m_{optic} = \frac{d \cdot (n - n_0)}{dn/dc} \quad (10)$$

Where d is the thickness of the adsorbed layer and n its refractive index, A is the sensitivity factor and dn/dc is the refractive index increment of the adsorbed material.¹⁶³ In this work a prototype instrument of combined QCM-D and reflectometry has been used. This enables the two techniques to be used simultaneously, at the same sensor surface, and the degree of hydration (H) to be determined.

$$H = \frac{m_{acoustic} - m_{optic}}{m_{acoustic}} \quad (11)$$

Summary of the appended papers

6.1 Brief summary of papers

In this thesis, interactions at the nano-bio interface are explored, an area of research that is currently intensively investigated.^{123, 164-166} The understanding of these interactions is of great importance from both a nanotoxicological and a nanomedical perspective. Interactions between certain nanomaterials and lipid bilayers, the main constituent of biological membranes, have been investigated in detail using surface sensitive analytical techniques. These techniques are further described in Chapter 5. In **Paper I and II**, the properties of engineered polyelectrolyte complexes (PECs) consisting of polycationic polymers and human insulin were investigated. Differently charged supported lipid membranes were exposed to these nano-sized PECs and it was shown that the interactions were mainly mediated by electrostatics. Furthermore, structural deformation of the PECs occurred upon adsorption to the lipid membranes, a process that was not expected by the researchers that developed these PECs. Engineered features of PECs (pH-sensitivity and sensitivity to a reductive environment) were also evaluated. In **Paper III**, the interactions between graphene oxide and lipid membranes were investigated. The results showed that graphene oxide adsorbed flat onto positively charged lipid membranes. Interestingly, it was proven possible to build multilamellar structures of graphene oxide and lipid membranes in a layer-by-layer fashion. Sequential addition of liposomes and graphene oxide resulted in the formation of additional lipid membranes with adsorbed graphene oxide. More specifically, the liposomes adsorbed intact on the graphene oxide surface and were ruptured by the graphene oxide upon the next addition. The resulting bio/nonbio nanocomposite structure may serve as a scaffold for the utilization of advanced biomolecular functions. In **Paper IV**, TiO₂ NPs, commonly used in consumer products, were studied with respect to their lipid membrane interactions. It was found that these NPs induced rupture of POPG-containing lipid membranes. Furthermore, it was elucidated that the removal of lipid material was dependent on the presence of Ca²⁺ ions. Upon repeated, and sequential, addition of Ca²⁺ ions and TiO₂ NPs more lipids were extracted from the supported membrane. Subsequent addition of liposomes, restored the disrupted lipid membrane.

In the final part of this thesis the membrane model system was substituted for living cells. In this way, the complexity of the biological interface increased tremendously. By studying living cells it was no longer possible to address fundamental aspects regarding the lipid membrane upon nanoparticle exposure. However, it was now possible to address intracellular processes in real-time. In **Paper V**, *Xenopus laevis* (African clawed frog) melanophores were cultured on QCM-D sensor surfaces and the responses obtained upon transport of melanosomes (pigment granules) were characterized. In this paper the utilization of QCM-D to study melanophores was addressed both from a QCM-D and a cell biology perspective. The paper formed a basis to subsequent

experiments where the effect of nanomaterials to the intracellular transport processes was addressed.

6.2 Experimental platform for nanomaterial – lipid membrane interactions

The three main components in the applied experimental platform were nanomaterials, lipid molecules and surface sensitive analytical techniques. In addition, the nanomaterials were characterized using light scattering methods to determine their size distribution and zeta (ζ) potential. The first component, the nanomaterials, was selected based on two major factors, availability and suitability. Naturally, the nanomaterials had to be available in sufficient quantities to enable the analyses, either from collaborators or from commercial sources. In my research, I have not developed any nanomaterials on my own. In addition to the availability, the nanomaterials had to be suitable for *in vitro* studies, *i.e.*, they had to be well defined and synthesized in a reproducible manner. It has also been an aim to include studies of significantly dissimilar nanomaterials in this thesis. The second component, the lipid molecules, was chosen partly due to the presence in native cell membrane and partly due to their charge. By combining lipids of different net charge it was possible to tune the charge of the resulting lipid membrane. See section 4.1.2 for further details regarding lipid molecules. The third, and last, main component of the described experimental platform is the experimental techniques. Several methods were used to investigate the nanomaterial- lipid membrane interactions, these were: QCM-D, reflectometry, AFM and DPI. QCM-D was chosen to be the main method of analysis due to the gained structural information of the NP-SLB interactions and the relatively high throughput. In addition to QCM-D, techniques giving complementary information were applied to support the interpretation of the studied surface associated interaction processes.

In the following sections the results obtained in studies of insulin-loaded drug carriers, graphene oxide and TiO₂ NPs are described in some detail. Additional details are given in the appended papers.

6.2.1 Insulin-loaded drug carriers (Paper I and II)

In paper I and II, different insulin loaded PECs have been studied with respect to their lipid membrane interactions. Also, in the latter paper, functionalities of the PECs were evaluated. As a first step, all types of prepared PECs were characterized with respect to their size and charge. These types of analysis were mainly performed using dynamic (size) and electrophoretic (charge) light scattering. The preferred sample should have a low polydispersity and a low variation of the mean size between different batches. In Paper I, the investigated NP (referred to as NP-HI) was analyzed with both DLS and SEM (Figure 20). The hydrodynamic diameter was determined to approximately 220 nm by DLS. In contrast, the size revealed by electron microscopy was much smaller ($d < 100$ nm). The large difference between these results was due to the hydration of the analyzed NPs. Prior to the SEM analysis, the sample are dried and the analysis is preformed under vacuum conditions whereas the DLS analysis is preformed in

liquid. Naturally, these different sample preparations yield particles with different size.

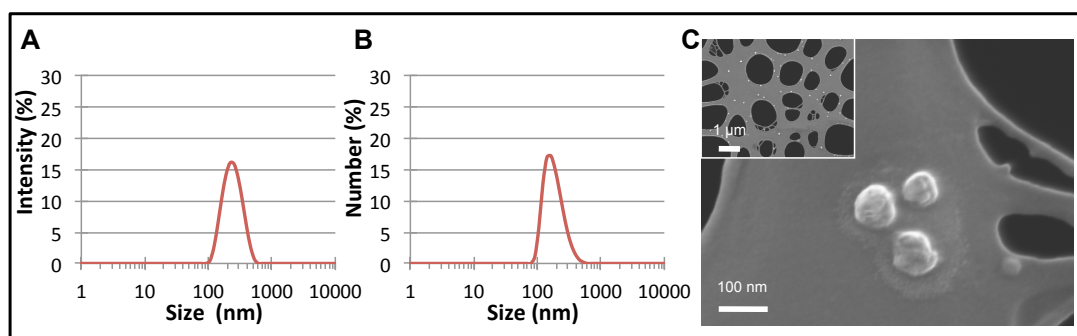


Figure 20. Characterization of NP-HI with respect to size. (A) Intensity and (B) number distributions obtained by DLS. (C) SEM images of different magnifications (20 000x (inset) and 400 000x) visualizing the studied NPs. (Paper I)

Apart from the presented example, all size characterizations of NPs were solely based on DLS analyses. This method was selected because of the possibility to perform the analyses under the same conditions as for the following QCM-D, reflectometry, and AFM experiments, as well as of the high throughput.

After the nanomaterials were characterized by light scattering techniques and it was concluded that the materials were well defined, their interaction with model lipid membranes were analyzed. Three model membranes, based on differently charged phospholipids, were used in paper I. SLBs were formed in PBS (pH 7.4) on a SiO₂ support using positively charged (ζ -potential: 22 ± 0.8 mV) POPC:POEPC (3:1), neutral/slightly negatively charged (ζ -potential: -0.3 ± 1.0 mV) POPC, and negatively charged (ζ -potential: -26 ± 1.2 mV) POPC:POPS (3:1) liposomes. In paper II, only the latter of these lipid compositions was used. For this negatively charged SLB, 5 mM MgCl₂ was added to the buffer to promote the bilayer formation process. The formed SLBs were assumed to have similar charge as the corresponding liposomes.

In a next step, NPs were added to the formed SLBs and the outcome of the NP-SLB interaction was studied in real-time with QCM-D. From the recorded data, specific experiments were selected to be further explored by the use of other surface based techniques, *e.g.* AFM or combined QCM-D/reflectometry. In paper I, NP-HI selectively interacted with the negatively charged POPC and POPC:POPS membranes. This was an expected result due to the positive charge of the NP-HI (ζ -potential: 26 ± 2 mV, pH 7.4). However, the QCM-D analysis showed that the adsorbed NP-HI had different structural confirmations depending on the degree of negative charge of the membrane. QCM-D responses obtained when NP-HI adsorbed on a negatively charged POPC:POPS (3:1) membrane suggested the formation of a thin and fairly rigid structure on the membrane. A more loose structure was formed on a plain POPC membrane. This layer was characterized by high ΔD values and by large spreading between different harmonics compared to the POPC:POPS (3:1) membrane (Figure 21).

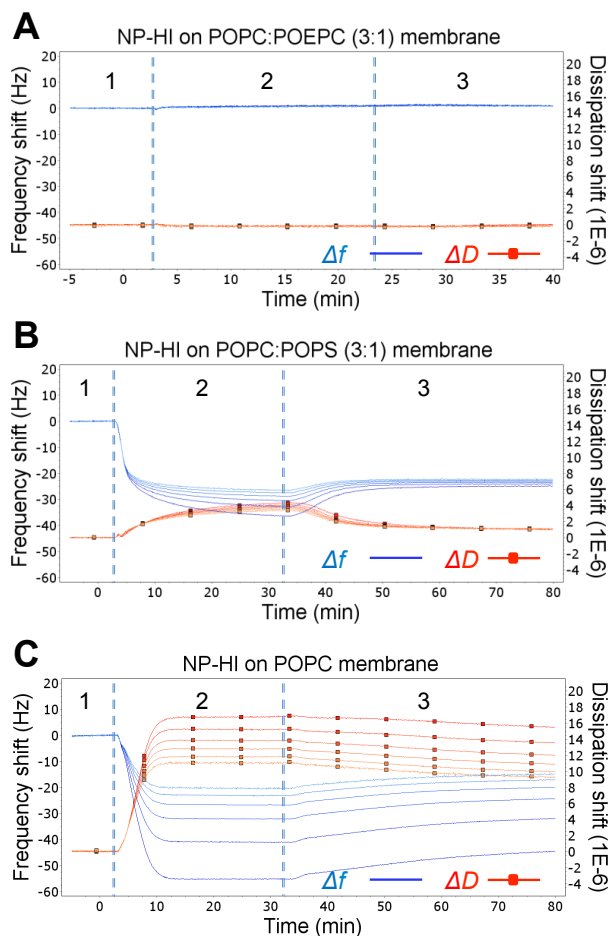


Figure 21. QCM-D data ($z = 3, 5, 7, 9, 11$ and 13) of the interaction between NP-HI and three differently charged model membranes. Larger frequency and dissipation shifts were obtained for lower overtone numbers. (A) Positively charged POPC:POEPC (3:1), (B) negatively charged POPC:POPS (3:1) and (C) slightly negatively charged POPC. The plots show a sequence of events including (1) baseline in buffer, (2) addition of NP-HI and (3) buffer rinse. The preceding steps of bilayer formation and buffer exchange were omitted in the plots. (Paper I)

To further investigate the structural differences between these two cases, they were analyzed in a combined QCM-D/reflectometry setup. The aim of this analysis was to compare the two different structural arrangements of the adsorbed NPs with respect to their degree of hydration. For NP-HI layers adsorbed on a POPC:POPS (3:1) membrane, m_{acoustic} and m_{optical} were calculated as described in section 5.2 and 5.5 respectively, and the degree of hydration was determined to approximately 70%. The thicker layer formed by adsorption of NP-HI to a plain POPC membrane generated a decrease in the optical signal (ΔR). At first this result seemingly suggests, in contrast to the QCM-D data that mass is lost from the surface. However, the negative optical signal was to be expected for thicker films of the adsorbed material, based on optical modeling of the system.

When NPs are taken up by a cell through endocytosis they are subjected to a low pH in the late endosome. This change in the surrounding environment can be utilized to trigger the release of the drug from its carrier. Similarly, the intracellular reductive environment can be used to disintegrate the carrier to promote drug release. In paper II, three different responsive PECs based on poly(amido amine)s were produced and evaluated. These NPs were responsive

to reducing agents due to the presence of disulfide linkages¹⁶⁷ in the backbone of the polymers. The NPs, which are referred to as NP 1-3, were also designed to disintegrate when pH was decreased from physiological to about 5 due to a strong decrease in the charge attraction between the polymer and the protein at this low pH. In this study, the NPs were first adsorbed to a preformed POPC:POPS (3:1) membrane. Subsequently, the ambient conditions were altered either by adding a reducing agent (glutathione) or by decreasing the pH. As expected, NPs containing disulfide linkages in the polymer backbone responded to the presence of glutathione while the NP without disulfide linkages was unaffected by the addition of glutathione. The previously adsorbed NPs containing disulfide linkages dissociated from the membrane. The QCM-D frequency shift Δf suggested that the intact lipid membrane remained on the surface. The percent of the adsorbed NP mass that dissociated from the surface in the three different cases are presented in Figure 22A.

In addition, NP 1 was evaluated with respect to its pH-sensitivity. After adsorption to a POPC:POPS membrane and subsequent buffer rinse, the pH was decreased from 7.3 to 5.1 using a pH-gradient lasting for one hour. The result shows that mass start to dissociate from the surface at a pH of approximately 6.5. After this point, a rapid mass release occurs until a pH-value of about 6. Finally, at pH 5.1, the mass loss has leveled out at a level where 20 % of the initial amount of mass is left on the membrane. The result is presented in Figure 22B.

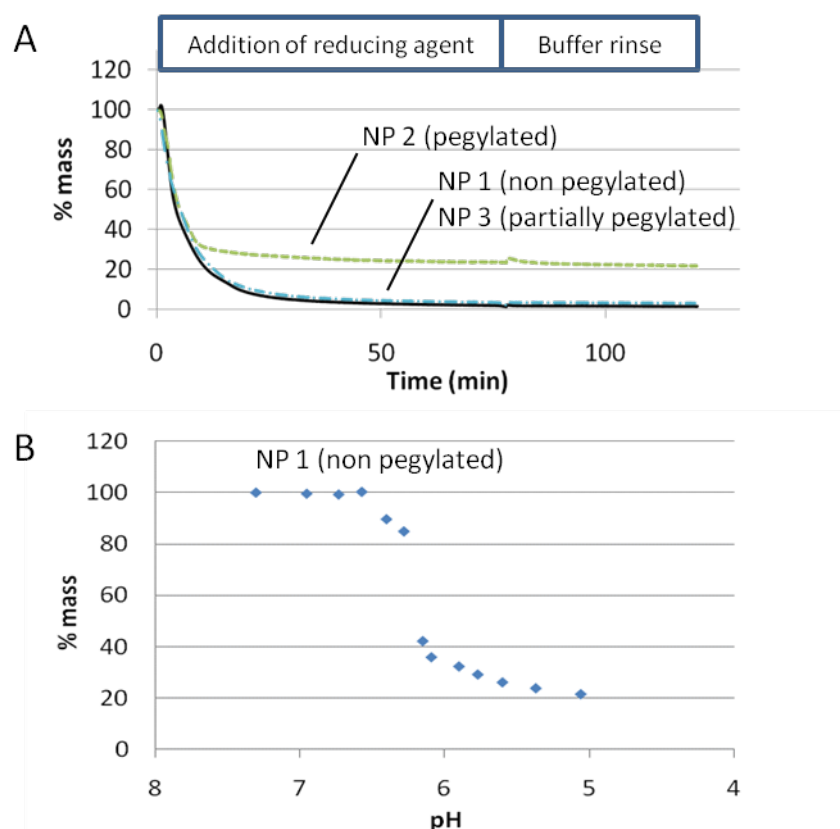


Figure 22. Response of the adsorbed NPs to (A) addition of a reducing agent (glutathione) and (B) a decrease in pH. (Paper II)

The scenario suggested by the interpretation of the QCM-D data was further strengthened by AFM measurements. The adsorption of NP 1 to the model

membrane and its response to glutathione was evaluated by imaging after the formation of the SLB, after adsorption of NPs, and after addition of glutathione (Figure 23). Corresponding force spectra were also recorded. The bare SLB was detected by a kink in the force spectrum originating from when the tip was pressed through the SLB during its approach towards the surface. After adsorption of NP 1, this characteristic kink corresponding to the SLB was still present. In addition, forces were exerted on the tip several tens of nanometers away from the surface. This event in the force spectrum reveals the presence of the adsorbed NP material. Another main difference in the force spectrum after addition of NPs was the pull off force. Before addition of NPs the pull off was a distinct event where the tip snapped off the surface, while after addition of NPs the pull off occurred much more slowly. After addition of glutathione two different regions were revealed on the surface. Although the SLB could be detected in both, the force spectra suggested that in one of the regions an additional thin layer of NP material was present.

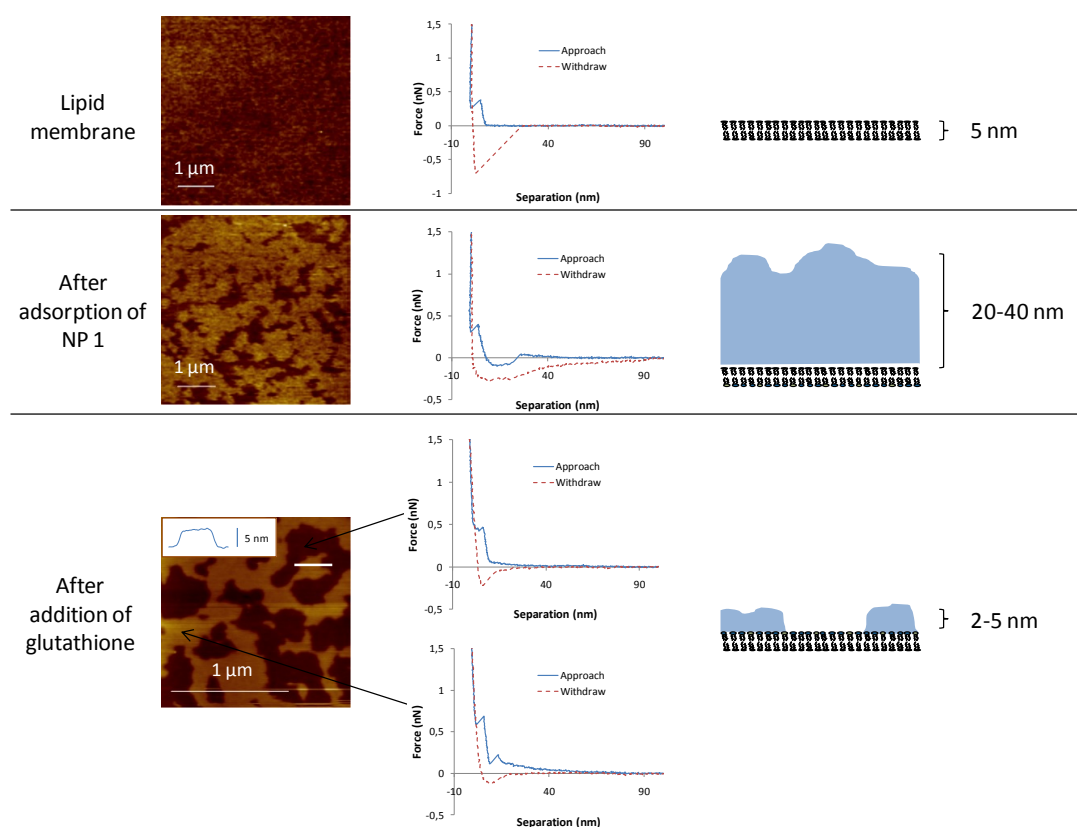


Figure 23. AFM images, corresponding force spectra and schematic models (not to scale) of the bare lipid membrane (z-range 1.6 nm), after adsorption of NP 1 (z-range 3.0 nm) and after addition of glutathione (z-range 10 nm). The cross section, shown in the inset, corresponds to the white bar in the image. (Paper II)

By combining the data obtained from QCM-D and AFM after NP adsorption and after subsequent addition of glutathione, a schematic model of the surface was made. The model, which is shown to the right in Figure 23, shows that the NPs collapse into a layer much thinner than the hydrodynamic diameter of the NPs ($d = 165 \pm 5$ nm) when adsorbed to a POPC:POPS membrane. After addition of glutathione only a few nanometers thick layer which partially covered the

surface remained. Both the presented cases where adsorbed NPs dissociate from the surface due to particle disintegration were most likely associated with release of the insulin drug load. However, to follow the release of insulin from its carrier other methods must be applied which in most cases require labeling of the insulin molecules.

6.2.2 Graphene oxide (Paper III)

In paper III, QCM-D analyses show that graphene oxide adsorb selectively to positively charged supported lipid membranes (POPC:POEPC (3:1)), *i.e.*, the interactions are mainly due to electrostatic forces. The magnitude of the observed frequency shifts corresponded well to the predicted shift of an adsorbed monolayer of graphene oxide (~ -6 Hz). Furthermore, the absence of a response in dissipation upon adsorption indicated that the graphene oxide flakes adsorbed flat onto the lipid membrane. These results were further supported by the DPI analyses where the dry mass of the adsorbed graphene oxide and its birefringence were determined. By comparing the mass determined by QCM-D and DPI the hydration level of the graphene oxide layer was determined to 32%. Such difference in mass is commonly observed when comparing acoustically and optically derived data. More noteworthy is the observed negative birefringence of the graphene oxide layer. The origin of the negative birefringence is the larger polarizability of the adsorbed graphene oxide in the plane parallel to the sensor surface compared to the direction normal to that plane. In Figure 24, the anisotropic properties of both the lipid membrane and the layer of graphene oxide are evident through the difference between the transverse magnetic (TM) and transverse electric (TE) responses. TM and TE are two orthogonal polarizations of the incident light. See section 5.4 for further details regarding the DPI technique. For isotropic materials TM is always larger than TE, however in the case of graphene oxide adsorbed to a lipid membrane the situation was reversed. This unusual scenario yielded a negative birefringence.

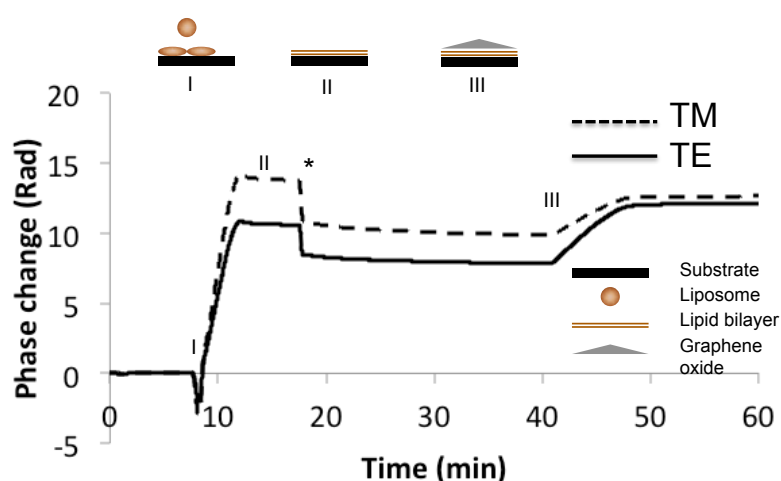


Figure 24. DPI data recorded during (I-II) the formation of a supported lipid membrane, (*) a subsequent liquid exchange from PBS to water and (III) the adsorption of graphene oxide.

Once the addition of graphene oxide reached saturation the surface was, at least to some extent, covered with that material. At that point, it became possible

to investigate how liposomes interacted with a graphene oxide coated surface. Since the liposomes were of the same lipid composition as the underlying lipid membrane, possible interactions were only expected at the areas covered with graphene oxide. The result showed that POPC:POEPC (3:1) liposomes adsorbed intact on top of the graphene oxide flakes. This result was clearly evident due to the large positive dissipation shift upon addition of liposomes. However, if graphene oxide was added to the intact liposomes the high dissipation returned to a very low level, indicating that graphene oxide induced rupture of the liposomes. The additions of liposomes and graphene oxide were cycled up to three times and for each cycle more material was deposited at the surface in a layer-by-layer fashion. The QCM-D and DPI data of the multilayer buildup are shown in Figure 25.

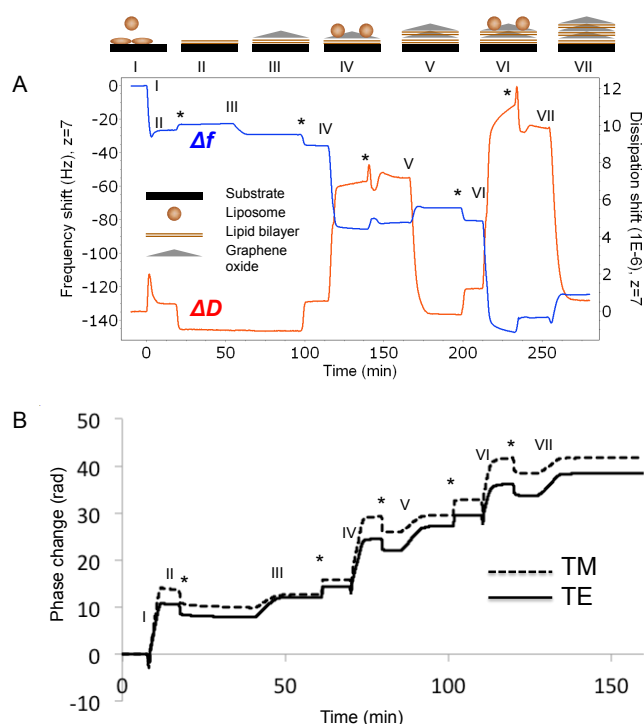


Figure 25. (A) QCM-D data showing the sequential build-up of a multilayered structure of POPC/POEPC (3:1) membranes and graphene oxide, starting from (I) the adsorption of liposomes to a silica surface and (II) the spontaneous formation of a supported lipid membrane. Next, (III) graphene oxide is added, followed by (IV and VI) additional injections of liposomes and (V and VII) of graphene oxide. The additions of graphene oxide and liposomes are preceded by a (*) liquid exchange to water and PBS respectively. (B) DPI data of the same processes as in (A).

Upon the graphene oxide induced rupture of liposomes it was hypothesized from the QCM-D data that a lipid bilayer was formed in between the graphene oxide flakes, as schematically shown in Figure 26. However, from the QCM-D responses alone it was not possible to verify this. As a complement, AFM analyses were performed to image the sample surfaces during and after the formation of the multi-lamellar structure.

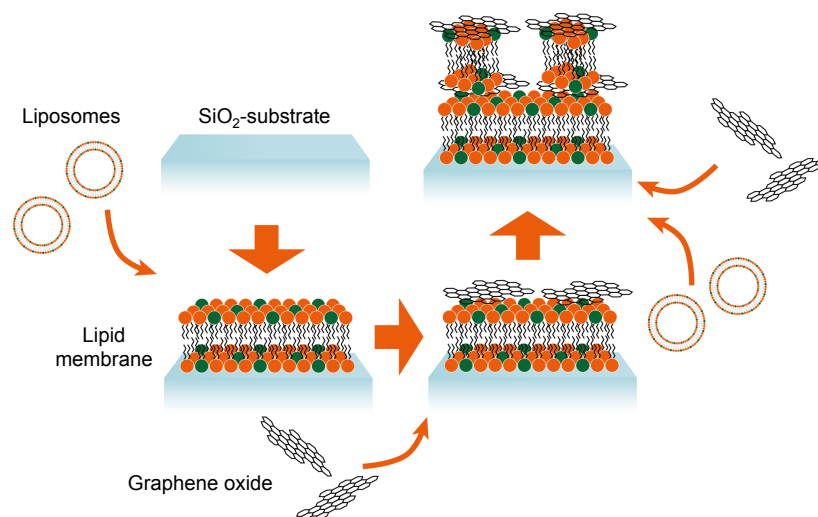


Figure 26. Schematic representation of the buildup of a multilayered structure consisting of POPC:POEPC (3:1) lipid bilayers and graphene oxide.

In the AFM images, presented in Figure 27, adsorbed graphene oxide flakes were visualized, both after the first addition and after three additions. When analyzing the images recorded after three cycles of added liposomes and graphene oxide, it was revealed that some specific heights occurred more frequently than others on the surface. We interpreted these heights to be multiples of a lipid bilayer with adsorbed graphene oxide.

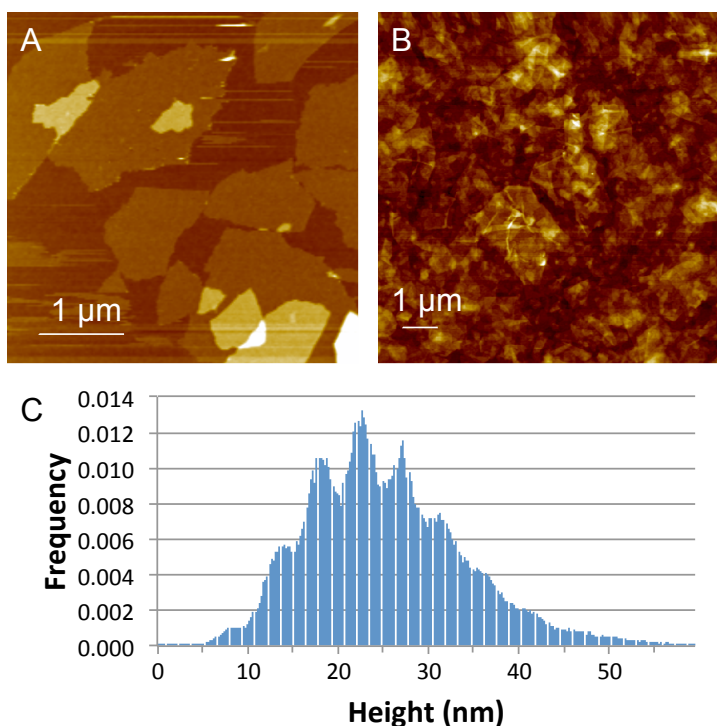


Figure 27. (A) AFM image of graphene oxide adsorbed to a POPC:POEPC (3:1) lipid membrane. The image was recorded in water (z-range: 29 nm). (B) AFM image of the multilayered structure consisting of lipid bilayers and graphene oxide. The image was recorded after three cycles of added liposomes and graphene oxide and after the structure has been dried (z-range: 81 nm). (C) Histogram of the height profile in (B).

Taken together, paper III presents data on the interactions between graphene oxide and supported lipid membranes as well as supported liposomes. Also the reverse situation, where a surface coated with liposomes was exposed to graphene oxide, was explored. In addition, the formation of a novel nanocomposite structure consisting of alternating layers of lipid membranes and graphene oxide was shown.

6.2.3 TiO₂ nanoparticles (Paper IV)

In paper IV, supported lipid membranes composed of POPC and POPG lipid molecules were exposed to TiO₂ NPs of about 60 nm. J.P. Holmberg synthesized these NPs via hydrolysis of TiCl₄.¹⁶⁸ The synthesis took place in an acidic environment and produced particles in the size range of 7-20 nm. The size of the NPs increased to around 60 nm during the subsequent shift in pH, from 2.5 to 8. The main crystal structure of these NPs was anatase.

F. Zhao exposed POPC:POPG (1:1) supported lipid membranes to the synthesized TiO₂ NPs. The QCM-D data indicated that the membranes were disrupted by the NP exposure, a process that was dependent on the presence of Ca²⁺ ions. Upon repeated exposures and additions of Ca²⁺, more and more lipid mass was removed from the sensor surface. In my analyses, I confirmed the presence of holes in the lipid membrane after exposure to the TiO₂ NPs. In the AFM images, holes much larger than the size of the NPs were observed. This was most likely due to the fluidity of the lipid membrane. When small holes are formed the lipids rearrange to a more energetically favorable state and in this process the small holes merge into larger ones. In the AFM analyses the lipid membrane was detected by force spectroscopy. This method was also used to probe the absence of the lipid membranes in the observed holes. The height profile of the holes corresponded well to the expected thickness of a lipid membrane (about 5 nm).

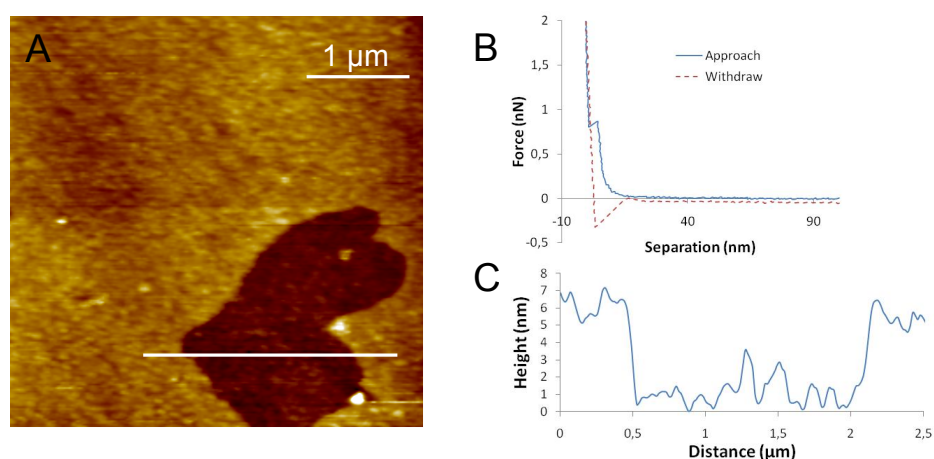


Figure 28. (A) AFM image (z-range 20.9 nm) of a hole in a POPC:POPG (1:1) lipid membrane on a QCM-D crystal. The dark area corresponds to the hole while the brighter area corresponds to the lipid membrane. (B) Force spectra recorded on the lipid membrane. The kink in the spectra during the approach indicates the presence of a lipid membrane. (C) Height profile according to the white line in (A).

6.3 Monitoring of intracellular transport by QCM-D (Paper V)

In paper V, the use of QCM-D to detect and monitor the translocation of melanosomes in *Xenopus laevis* melanophores was explored. If possible, QCM-D may be used to monitor changes of intracellular transport processes upon nanomaterial exposure. The results showed significant responses in both Δf and ΔD upon melanosome transport induced by MSH or melatonin (Figure 29). Thus, QCM-D is a new tool to be used in the studies of melanophores and of intracellular transport processes. In this thesis, the use of melanophores is an extension of the experimental platform described in section 6.2, *i.e.* the well-defined lipid membranes used in paper I-IV were substituted to living cells. With this substitution the complexity of the system increased tremendously, however real-time studies of intracellular processes was enabled.

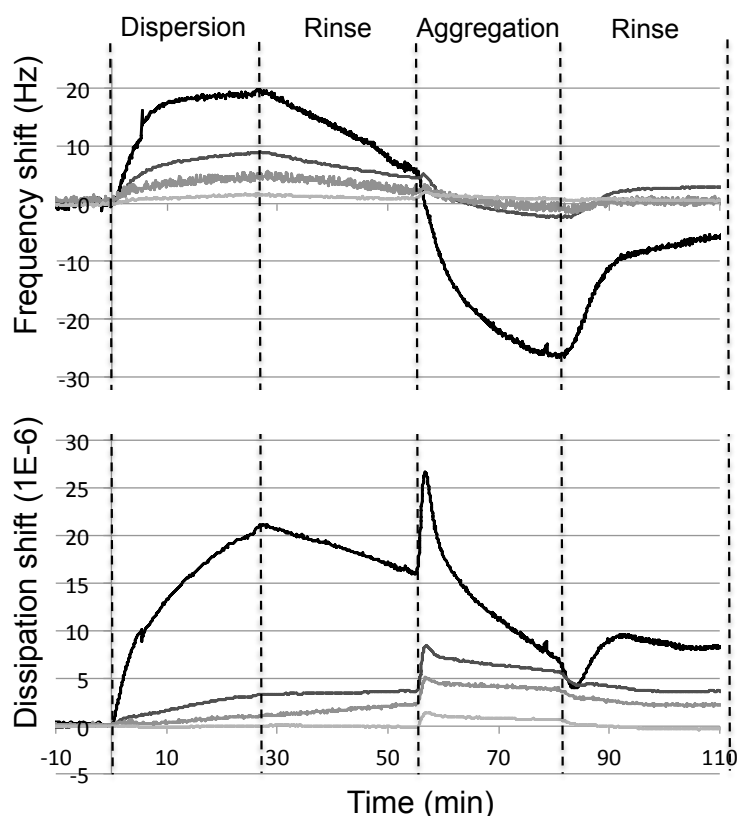


Figure 29. QCM-D responses recorded during the sequential process of melanosome dispersion (induced by 100 nM MSH), medium rinse, melanosome aggregation (induced by 10 nM melatonin), and medium rinse. A selection of harmonics ($z=1, 3, 5,$ and 9), where the lower harmonics give rise to greater responses, is shown.

Before studying possible effects of nanomaterial exposure to the melanophores it was important to better characterize the origin of the observed responses during melanosome transport. This was performed in the following four ways. First, the recorded QCM-D responses were correlated to the reflectance of the melanophores at the surface during melanosome dispersion and aggregation. Second, the synthesis of melanin (the pigment enclosed inside the melanosomes) was blocked by phenylthiocarbamide (PTC). The resulting

“bleached” melanophores, *i.e.* melanophores lacking pigment, were then compared to untreated melanophores in QCM-D analyses. Third, the melanosome transport was studied upon disruption of cytoskeletal filaments (actin filaments and microtubules). When breaking down these structures, transport along such filaments was prohibited. Last, the vertical redistribution of melanosomes upon dispersion and aggregation was studied by confocal microscopy.

Dispersed melanosomes makes the skin of the animal darker compared to when the melanosomes are in an aggregated state, *i.e.*, the melanophores absorb more light in the former case. For this reason, the reflectance of the cell-coated surface was measured simultaneously as the QCM-D responses. The results presented in Figure 30, clearly showed that the observed shift in frequency correlated well with the reflectance of the sample surface. Hence, the frequency shift correlates well to the state of melanosome distribution.

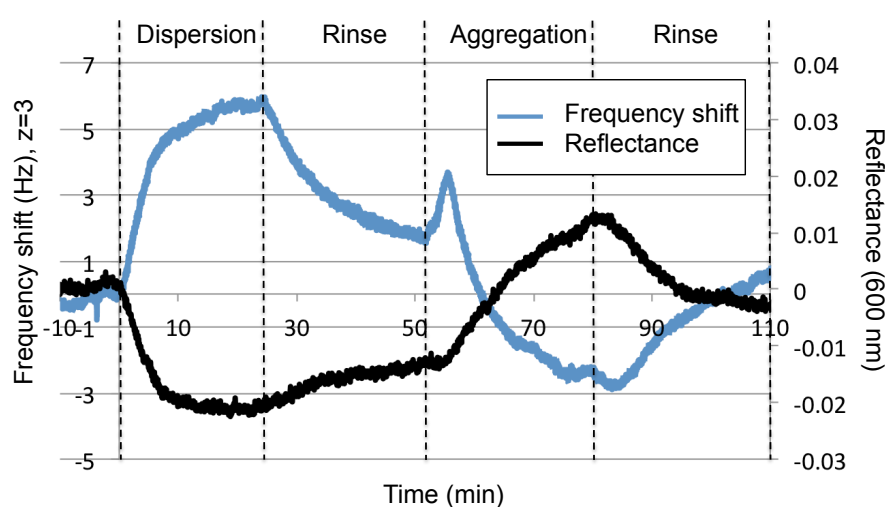


Figure 30. QCM-D and reflectance data recorded simultaneously during melanosome dispersion and aggregation.

Repeating the experiment presented in Figure 29, where dispersion and aggregation of melanosomes was induced, resulted in significantly lowered responses when using depigmented melanophores. This result showed that the observed responses to a large extent originated from the presence of melanin. It has not been established if the blocked synthesis of melanin also hinders the formation of melanosomes. Possibly, empty melanosomes may still be transported in the cytosol. If so, the mass of the melanin would be the major contributor to the observed QCM-D responses.

In the third way of elucidating the origin of the observed QCM-D responses, the melanophores were either exposed to latrunculin or nocodazole. These substances efficiently disrupt the actin filaments (latrunculin) or the microtubules (nocodazole). Since these effects are reversible, the dispersion-aggregation cycle was performed prior to addition, and in presence, of the two substances. When the cells were exposed to latrunculin, large shifts in both frequency and dissipation were observed (Figure 31). This was an expected observation since disruption of the actin filaments changes the morphology of the cells and how they adhere to the substrate. Also, this event causes aggregation of melanosomes in the cell center. However, the subsequent addition

of MSH did not yield a response. This is in accordance with the fact that dispersion of melanosomes occurs along actin filaments. If no such filaments are present, melanosomes cannot be transported to the cell periphery. Aggregation however, which takes place along microtubules, still yielded a detectable response. In the case of nocodazole, there were no significant responses in Δf and ΔD upon addition. Surprisingly, the responses during the dispersion and aggregation cycle in the presence of nocodazole were similar to the one prior to the addition (Figure 31). Seemingly, the observed responses did not originate from transport along microtubules. Taken together, the results indicate that the response recorded during dispersion is due to melanosome transport along actin filaments. However, the data do not clarify the origin of the response during melanosome aggregation.

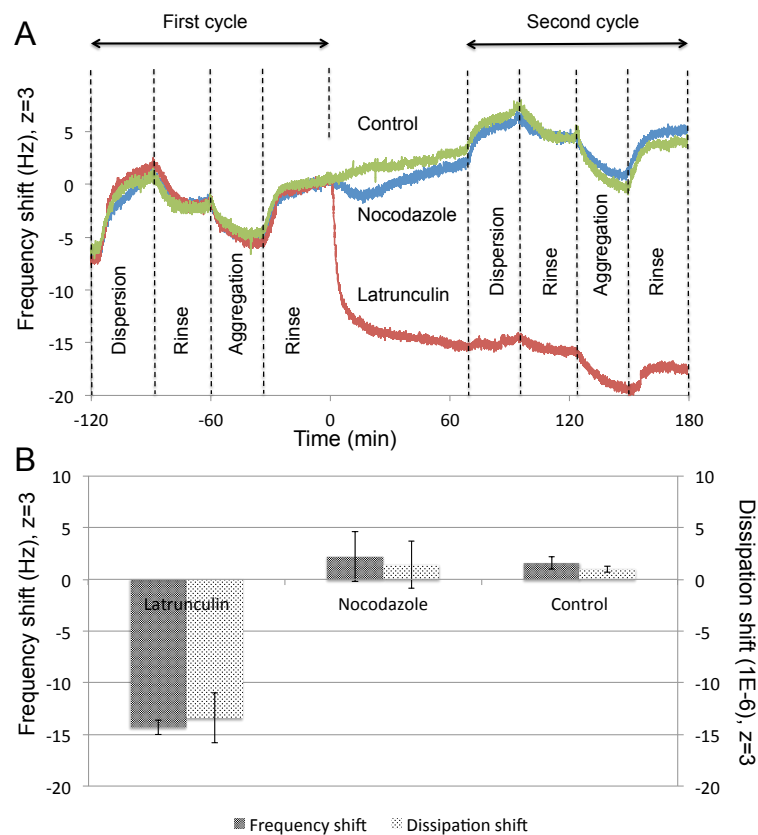


Figure 31. (A) QCM-D Δf responses of the dispersion-aggregation cycle in the absence and presence of latrunculin and nocodazole. (B) Δf and ΔD responses upon addition of latrunculin and nocodazole compared to untreated cells.

In paper V, the origin of the observed QCM-D responses is also discussed with respect to the penetration depths of the different harmonics included in the analyses ($z = 1, 3, 5, 7, 9, 11,$ and 13). The results indicated that mainly the first and third harmonics sensed the dispersion and aggregation processes. One explanation for this is that only these harmonics penetrate sufficiently deep into the cells to probe the transport processes. In such scenario, higher harmonics will only sense the cell-substrate interface. Due to the cell morphology it is reasonable to believe that a larger number of melanosomes will be positioned close to the sensor surface in the dispersed state compared to the

aggregated state. In the latter state, the melanosomes are clustered deeper into the cell. Thus, one model for the origin of the QCM-D responses is given as follows. Transport of melanosomes to and from a volume close to the sensor surface, covered by the first and third harmonics, give rise to detectable QCM-D responses.

The distribution of melanosomes in the dimension extending out from the substrate (z-dimension) was analyzed by confocal microscopy. The results show that there was a distinct difference in the melanosome distribution in the z-dimension, between the dispersed and aggregated state (Figure 32). In the dispersed state there was a large number of melanosomes close to the sensor surface compared to the aggregated state. Thus, the distribution of distances between the melanosomes and the substrate differs significantly between the dispersed and the aggregated state. These data support the reasoning that it is the transport of melanosomes to and from a volume close to the sensor surface that generate the observed QCM-D responses.

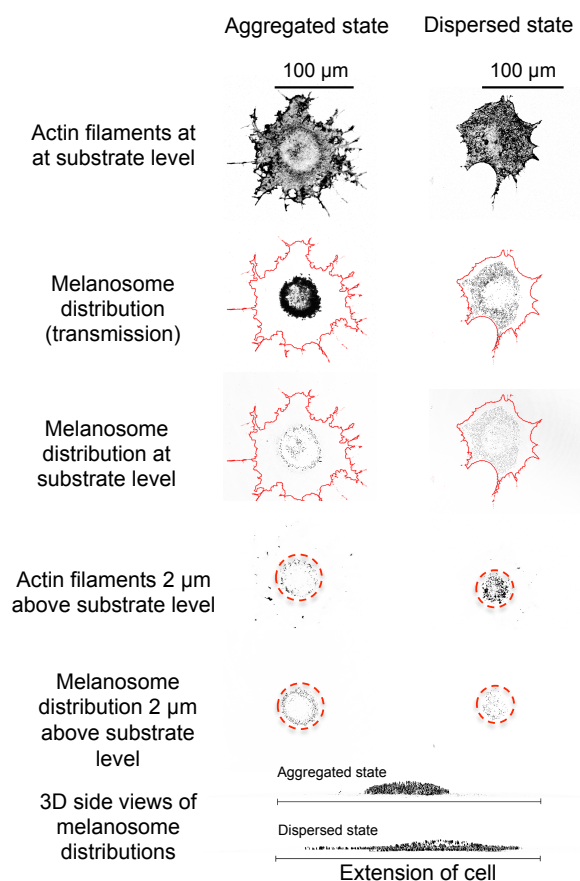


Figure 32. The figure shows confocal microscopy images of two melanophores, one in the aggregated state (left column) and the other in the dispersed state (right column). For each of these two states the actin filaments, and hence the footprints of the cells, are shown in a plane close to the substrate. In the same plane, and in a plane 2 μm above, the melanosome distributions are shown. For comparison, transmission images and 3D side views of the melanosome distributions of the two cells are included.

6.3.1 Effects of SiO₂ nanoparticle exposure (Additional results)

As a continuation of the work presented in Paper V, experiments where the melanophores were exposed to SiO₂ NPs were performed. These experiments may be seen as further downstream *in vitro* characterization of nanomaterials compared to the previously presented studies of model lipid membranes. In these experiments, the complexity of the system is much greater than in the well controlled interaction experiments using lipid membranes. A series of SiO₂ NPs was obtained from EKA chemicals (Bohus, Sweden), a company that produces large quantities of SiO₂ NPs for use in paper products. Due to the large volume produced and the various surface functionalizations available, these NPs were chosen to be used in the present experiments. The set of SiO₂ NPs consisted of clean (uncoated) NPs, NPs functionalized with isobutyl-groups (iBu), or PEG and isobutyl-groups (PEG/iBu), and rod-shaped NPs composed of smaller SiO₂ NPs (Figure 33). According to specifications, the spherical NPs had a diameter of 20 nm while the smaller NPs in the SiO₂-rods had a diameter of 3-4 nm (determined from titration of the specific surface area). The length of the rod shaped NPs was about 20 nm. However, the hydrodynamic diameters of the spherical NPs were determined to about 40 nm by DLS, when diluted in water. The size distributions are shown in Figure 33. By using this set of NPs it was possible to address both the effects of surface functionalization and to compare spherical NPs to NPs with high aspect ratio. Generally, high aspect ratio nanoparticles, *e.g.* nanotubes, nanorods, nanowires, and nanofibers, are considered more toxic than their spherical counterparts.¹⁶⁹ The main reason for this is the resemblance to asbestos fibers.

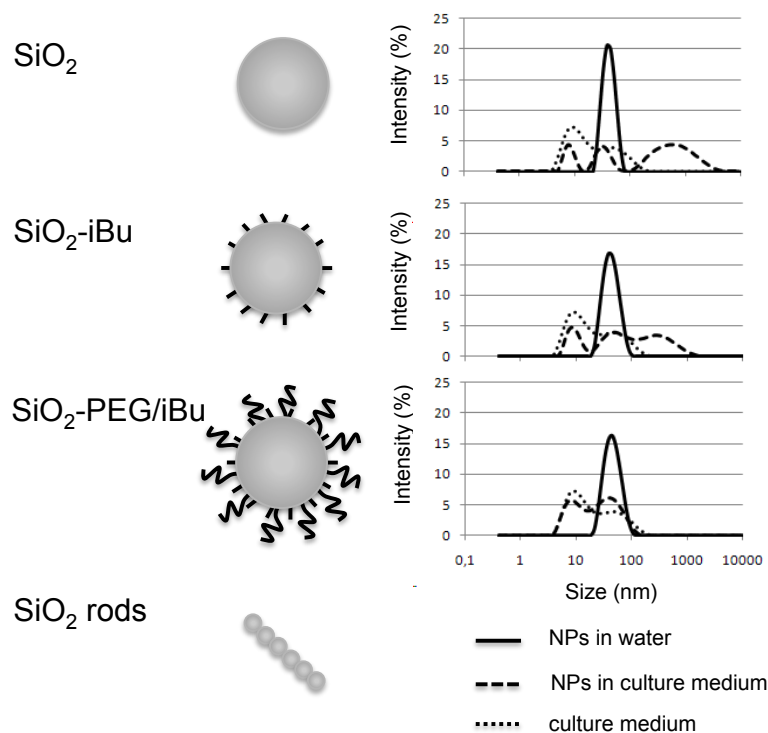


Figure 33. Set of SiO₂ NPs used in cell exposure experiments. The figure shows schematic representations of the NPs and the size distributions of the spherical NPs (by DLS) in water and in serum containing culture medium.

Xenopus laevis melanophores, pre-cultured on QCM-D sensor surfaces, were exposed to the SiO₂ NPs (50 µg/mL, 24 h) *ex situ*. The exposure was performed in serum containing culture medium. It is important to note that the added NPs will, depending on their functionalization, adsorb serum proteins and possibly aggregate/agglomerate in the culture medium. To analyze these effects, the NPs were studied by DLS when diluted to 50 µg/mL in water and culture medium respectively. The preliminary results are presented in Figure 33. Subsequently, the sensors were mounted in a QCM-D E4 instrument and the intracellular transport of melanosomes was sequentially induced by MSH and melatonin. The recorded shifts during melanosome dispersion and aggregation of the exposed cells were then compared to responses obtained using unexposed control cells. By this methodology it is possible to probe the impact of NP exposure on melanosome transport processes. If an effect of NP exposure would be observed, the next step may be to expose the cells *in situ*, during a QCM-D analyses, and possibly detect a response in real-time. Here, the response during dispersion of melanosomes was chosen as an experimental endpoint. The results showed a significant variation of the responses between different replicates, including the unexposed control (Figure 34). One likely explanation for this is the variation of the starting material. It is not certain that the cell density and the cell adhesion to the substrate were similar between the different replicates, although the same number of cells was seeded and the culture time was kept the same. Despite the variation in result between different experiments, there are some indications in the obtained data. Exposure to the SiO₂ rods gave hampered responses during melanosome dispersion compared to the responses of the unexposed control cells. In contrast, cells exposed to the iBu/PEG-coated SiO₂ NPs generated large responses in the same process. When comparing the results of these two exposures there were significant differences between the recorded QCM-D responses. These differences indicated that primarily the shape of the SiO₂ NPs had an impact on the melanosome transport process.

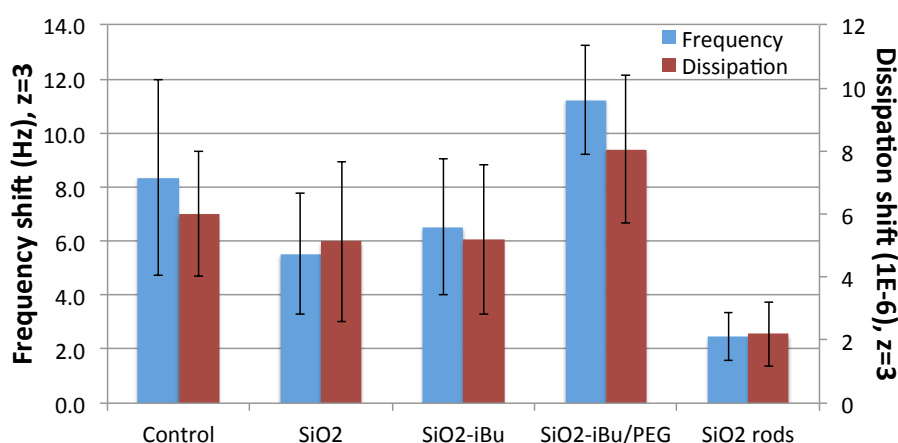


Figure 34. Average QCM-D responses during melanosome dispersion in melanophores exposed to SiO₂ NPs. The data in the figure is based on the following number of experiments. Control: six replicates; SiO₂, SiO₂-iBu, and SiO₂-iBu/PEG: four replicates; SiO₂ rods: two duplicates.

Concluding remarks and future perspectives

In brief, this thesis has contributed to the development of *in vitro* characterization methods for engineered nanomaterials. The presented data show the kind of information that may be extracted by studying the interactions between nanomaterials and model lipid membranes using surface based analytical techniques, both regarding the intrinsic properties of the nanomaterials and the effects exerted on the lipid membranes. Furthermore, this thesis has extended the use of the QCM-D technique to detection of intracellular transport processes. This possibility enables studies focusing on the effect of nanomaterials on such processes.

One key point that is of great significance for this work is the Janus-faced nature of nanomaterials. On one hand, the unique properties of these materials are promising for a wide range of applications. While on the other hand, the increased use and production volumes of nanomaterials pose a potential risk for adverse effects on the human health or the environment. As in the last decades, the future development of engineered nanomaterials will most likely continue. Due to this, it is of most importance that we learn to take advantage of the benefits that nano-sized materials bring in a safe and responsible manner. To accomplish this, there is a need for a definite definition of what a nanomaterial is. Such definition would enable legislation against potentially hazardous nanomaterials and make labeling of commercial products that contain nanomaterials possible. However, there is also a need for methodologies for better characterization of nanomaterials. The characterization process may be seen as a screening hierarchy that starts with the basic physico-chemical properties and ends with *in vivo*-studies. The large number of descriptors of a nanomaterial, compared to a chemical compound, put high demands on the characterization already at an early stage. The studies presented in this thesis, where nanomaterial-lipid membrane interactions were investigated, may be seen as an intermediate characterization step in the screening hierarchy. Upstream of these analyses is the physico-chemical characterization, and downstream comes *in vitro* cell assays and *in vivo* testing. I believe that there is a need for novel characterization techniques and methodologies at many stages in the screening process. Possibly, additional intermediate steps could be added to the mentioned hierarchy for a more thorough characterization. Due to the versatility of engineered nanomaterials the strategy adopted by OECD, to intensively study few selected nanomaterials and extrapolate the results to others by SARs, is crucial. From the risk perspective, it is necessary that the knowledge of potential hazards of a novel nanomaterial is sufficient prior to its use in commercial products. To achieve this, the risk assessment needs to progress rapidly.

The model lipid membranes that were used in the studies presented in this thesis could be viewed in two different ways. Either they are seen as very simple

models of a native cell membrane, or as model surfaces with tunable properties (by changing the lipid composition). In the first case, future efforts could be put in preparing more native-like model cell membranes at surfaces. This may be achieved by either a bottom-up approach, where membrane constituents subsequently are inserted into the supported lipid membrane, or a top-down approach, where native cell membranes are extracted and put on the surface. Neither of these approaches is trivial to pursue but they would both be valuable for research in this and other areas. If the lipid membranes are seen from a different perspective, as well defined model surfaces, the surface based analyses of nanomaterial interactions may be directly applied as a characterization tool for these materials. Obtained data from lipid membrane interaction studies may also be used to evaluate engineered nanomaterials and aid further development thereof.

The use of acoustic sensing in cell studies is increasing. However, there is still much to learn regarding interpretation of the acquired data. Cell attachment, spreading, and proliferation on surfaces could be evaluated using such sensing techniques but merely on a qualitative basis. There is a need for the development of theoretical models to extract quantitative information from the analyses, *e.g.*, on the viscoelastic properties of the cells. Such models may also predict possible effects of the surface coating on the recorded responses. At the same time as more work is needed to interpret and model data, there is also a need for further development of the instruments. The possibility to combine *e.g.* QCM-D and fluorescence microscopy would facilitate interpretation of the acoustic data. Generally, combining an acoustical and an optical sensing technique derive much information from the system under study. For this reason, more analytical techniques will most likely be combined to allow simultaneous measurements. A specific example recently initiated in my research project aims to combine QCM-D and localized surface plasmon resonance (LSPR) to probe cellular processes. I believe that the possibility to investigate cellular responses in real time will enable a continued development in this area of research. This type of studies will most likely become important for *in vitro* characterization of nanomaterials.

Acknowledgements

Many people have contributed to the work presented in this thesis and made my years as a PhD-student a joyful and educative experience. First of all, I would like to express my gratitude to my supervisor Sofia Svedhem for your encouragement and support throughout these years. Your positive attitude and contagious enthusiasm have been (and still are) truly inspiring. I am also very grateful to my examiner Fredrik Höök for giving me the opportunity to become a member of the division of Biological Physics, I am very happy that I ended up in your group. I would also like to thank Bengt Kasemo for valuable discussions regarding future experiments and prompt feedback on manuscripts.

I would like to acknowledge my collaborators, and co-authors, in Sweden and abroad. A special thanks to Christian Grandfils (University of Liège), Johan Engbersen and Gregory Coué (TWENTE University) for providing nanodrug formulations for the work resulting in paper I and II. I would also like to thank Dinko Chakarov for being part of the initiation of my work with graphene oxide, resulting in paper III. More recently, I have had the pleasure to collaborate with Elisabeth Norström, Lovisa Bodin, Joachim Sturve and Margareta Wallin at the department of Biological and Environmental Sciences (Gothenburg University), a collaboration that generated paper V. I am very grateful for the efforts you put into our project, I have learnt a lot from it.

Many thanks to the present and former members of the division of Biological Physics, you have created a nice group atmosphere and made the work enjoyable.

I gratefully acknowledge the funding obtained from the EU FP6 IP NanoBioPharmaceutics and the FORMAS project NanoSphere.

Finally, I would to give a special thanks to my wife Hanna for her love and support and to our wonderful children Elsa and Alfred.

References

1. Buzea, C., Pacheco, II, and Robbie, K. (2007) Nanomaterials and nanoparticles: Sources and toxicity, *Biointerphases* 2, MR17-MR71.
2. Duncan, R., and Gaspar, R. (2011) Nanomedicine(s) under the Microscope, *Mol. Pharm.* 8, 2101-2141.
3. Hughes, G. A. (2005) Nanostructure-mediated drug delivery, *Nanomedicine: Nanotechnology, Biology and Medicine* 1, 22-30.
4. Schrama, D., Reisfeld, R. A., and Becker, J. C. (2006) Antibody targeted drugs as cancer therapeutics, *Nat Rev Drug Discov* 5, 147-159.
5. Nel, A., Xia, T., Madler, L., and Li, N. (2006) Toxic potential of materials at the nanolevel, *Science* 311, 622-627.
6. Mossman, B. T., Bignon, J., Corn, M., Seaton, A., and Gee, J. B. L. (1990) Asbestos - scientific developments and implications for public-policy, *Science* 247, 294-301.
7. Dockery, D. W., Pope, C. A., Xu, X. P., Spengler, J. D., Ware, J. H., Fay, M. E., Ferris, B. G., and Speizer, F. E. (1993) An association between air-pollution and mortality in 6 United-States cities *New Engl. J. Med.* 329, 1753-1759.
8. Brunekreef, B., and Holgate, S. T. (2002) Air pollution and health, *Lancet* 360, 1233-1242.
9. Oberdorster, G., Oberdorster, E., and Oberdorster, J. (2005) Nanotoxicology: An emerging discipline evolving from studies of ultrafine particles, *Environ. Health Perspect.* 113, 823-839.
10. Oberdorster, G., Stone, V., and Donaldson, K. (2007) Toxicology of nanoparticles: A historical perspective, *Nanotoxicology* 1, 2-25.
11. Oberdorster, G., and Utell, M. J. (2002) Ultrafine particles in the urban air: To the respiratory tract - And beyond?, *Environ. Health Perspect.* 110, A440-A441.
12. Fuller, J. E., Zugates, G. T., Ferreira, L. S., Ow, H. S., Nguyen, N. N., Wiesner, U. B., and Langer, R. S. (2008) Intracellular delivery of core-shell fluorescent silica nanoparticles, *Biomaterials* 29, 1526-1532.
13. Roiter, Y., Ornatska, M., Rammohan, A. R., Balakrishnan, J., Heine, D. R., and Minko, S. (2008) Interaction of Nanoparticles with Lipid Membrane, *Nano Lett.* 8, 941-944.
14. Li, Y., Chen, X., and Gu, N. (2008) Computational Investigation of Interaction between Nanoparticles and Membranes: Hydrophobic/Hydrophilic Effect, *The Journal of Physical Chemistry B* 112, 16647-16653.
15. Peetla, C., and Labhasetwar, V. (2008) Biophysical characterization of nanoparticle-endothelial model cell membrane interactions, *Mol. Pharm.* 5, 418-429.
16. Leroueil, P. R., Berry, S. A., Duthie, K., Han, G., Rotello, V. M., McNerny, D. Q., Baker, J. R., Orr, B. G., and Holl, M. M. B. (2008) Wide varieties of cationic

- nanoparticles induce defects in supported lipid bilayers, *Nano Lett.* **8**, 420-424.
17. Hamada, T., Morita, M., Miyakawa, M., Sugimoto, R., Hatanaka, A., Vestergaard, M. C., and Takagi, M. (2012) Size-Dependent Partitioning of Nano/Microparticles Mediated by Membrane Lateral Heterogeneity, *J. Am. Chem. Soc.* **134**, 13990-13996.
 18. Castellana, E. T., and Cremer, P. S. (2006) Solid supported lipid bilayers: From biophysical studies to sensor design, *Surf. Sci. Rep.* **61**, 429-444.
 19. Keller, C. A., Glasmaster, K., Zhdanov, V. P., and Kasemo, B. (2000) Formation of supported membranes from vesicles, *Physical Review Letters* **84**, 5443-5446.
 20. Kunze, A., Sjövall, P., Kasemo, B., and Svedhem, S. (2009) In Situ Preparation and Modification of Supported Lipid Layers by Lipid Transfer from Vesicles Studied by QCM-D and TOF-SIMS, *J. Am. Chem. Soc.* **131**, 2450-2451.
 21. Boholm, M., and Boholm, A. (2012) The many faces of nano in newspaper reporting, *Journal of Nanoparticle Research* **14**.
 22. Roduner, E. (2006) Size matters: why nanomaterials are different, *Chemical Society reviews* **35**, 583-592.
 23. European Commission, Brussels (2011) Commission Recommendation of 18 October 2011 on the definition of nanomaterial, Official Journal of the European Union, L275, can be downloaded from <http://eur-lex.europa.eu/JOIndex.do>
 24. European Commission, Office for Official Publications of the European Communities, Luxembourg (2006) Nanomedicine: Drivers for development and possible impacts, can be downloaded from <http://ipts.jrc.ec.europa.eu/publications/pub.cfm?id=1745>
 25. Freestone, I., Meeks, N., Sax, M., and Higgitt, C. (2007) The Lycurgus Cup - A Roman nanotechnology, *Gold Bull.* **40**, 270-277.
 26. <http://www.nanotechproject.org>
 27. Novoselov, K. S., Geim, A. K., Morozov, S. V., Jiang, D., Zhang, Y., Dubonos, S. V., Grigorieva, I. V., and Firsov, A. A. (2004) Electric field effect in atomically thin carbon films, *Science* **306**, 666-669.
 28. Singh, V., Joung, D., Zhai, L., Das, S., Khondaker, S. I., and Seal, S. (2011) Graphene based materials: Past, present and future, *Prog. Mater. Sci.* **56**, 1178-1271.
 29. Compton, O. C., and Nguyen, S. T. (2010) Graphene oxide, highly reduced graphene oxide, and graphene: Versatile building blocks for carbon-based materials, *Small* **6**, 711-723.
 30. Huang, X., Qi, X., Boey, F., and Zhang, H. (2012) Graphene-based composites, *Chemical Society reviews* **41**, 666-686.
 31. Yin, Z., Wu, S., Zhou, X., Huang, X., Zhang, Q., Boey, F., and Zhang, H. (2010) Electrochemical Deposition of ZnO Nanorods on Transparent Reduced Graphene Oxide Electrodes for Hybrid Solar Cells, *Small* **6**, 307-312.
 32. Chen, S., Zhu, J. W., Wu, X. D., Han, Q. F., and Wang, X. (2010) Graphene Oxide-MnO₂ Nanocomposites for Supercapacitors, *Acs Nano* **4**, 2822-2830.

33. Lian, P. C., Zhu, X. F., Liang, S. Z., Li, Z., Yang, W. S., and Wang, H. H. (2011) High reversible capacity of SnO₂/graphene nanocomposite as an anode material for lithium-ion batteries, *Electrochimica Acta* 56, 4532-4539.
34. Qi, X., Pu, K.-Y., Li, H., Zhou, X., Wu, S., Fan, Q.-L., Liu, B., Boey, F., Huang, W., and Zhang, H. (2010) Amphiphilic Graphene Composites, *Angew. Chem. Int. Ed.* 49, 9426-9429.
35. Chang, H., Tang, L., Wang, Y., Jiang, J., and Li, J. (2010) Graphene Fluorescence Resonance Energy Transfer Aptasensor for the Thrombin Detection, *Anal. Chem.* 82, 2341-2346.
36. Mkhoyan, K. A., Contryman, A. W., Silcox, J., Stewart, D. A., Eda, G., Mattevi, C., Miller, S., and Chhowalla, M. (2009) Atomic and electronic structure of graphene-oxide, *Nano Lett.* 9, 1058-1063.
37. Wold, A. (1993) Photocatalytic properties of TiO₂, *Chemistry of Materials* 5, 280-283.
38. Linsebigler, A. L., Lu, G. Q., and Yates, J. T. (1995) Photocatalysis on tio2 surfaces - principles, mechanisms, and selected results, *Chemical Reviews* 95, 735-758.
39. Obare, S. O., and Meyer, G. J. (2004) Nanostructured materials for environmental remediation of organic contaminants in water, *Journal of Environmental Science and Health Part a-Toxic/Hazardous Substances & Environmental Engineering* 39, 2549-2582.
40. Oregan, B., and Grätzel, M. (1991) A low-cost, high-efficiency solar-cell based on dye-sensitized colloidal TiO₂ films, *Nature* 353, 737-740.
41. Gussman, N. (2005) We're history - Titanium dioxide: From black sand to white pigment, *Chem. Eng. Prog.* 101, 64-64.
42. Serpone, N., Dondi, D., and Albini, A. (2007) Inorganic and organic UV filters: Their role and efficacy in sunscreens and sun care product, *Inorganica Chimica Acta* 360, 794-802.
43. Arvidsson, R., Molander, S., and Sanden, B. A. (2012) Particle Flow Analysis Exploring Potential Use Phase Emissions of Titanium Dioxide Nanoparticles from Sunscreen, Paint, and Cement, *Journal of Industrial Ecology* 16, 343-351.
44. Diebold, U. (2003) The surface science of titanium dioxide, *Surf. Sci. Rep.* 48, 53-229.
45. Bergna, H. E., and Roberts, W. O., (Eds.) (2006) *Colloidal silica - Fundamentals and applications*, Vol. 131, Tayler & Francis Group, Boca Raton.
46. Organisation for Economic Co-operation and Development, Paris (2010) OECD Programme on the Safety of Manufactured Nanomaterials 2009-2012: Operational Plans of the Projects, Series on the Safety of Manufactured Nanomaterials No. 22, can be downloaded from <http://www.oecd.org>
47. Organisation for Economic Co-operation and Development, Paris (2010) List of manufactured nanomaterials and list of endpoints for phase one of the sponsorship programme for the testing of manufactured nanomaterials: revision, Series on the Safety of Manufactured Nanomaterials No. 27, can be downloaded from <http://www.oecd.org>
48. European Commission, Office for Official Publications of the European Communities, Luxembourg (2004) Communication from the Commission –

- Towards a European strategy for nanotechnology, can be downloaded from http://ec.europa.eu/nanotechnology/policies_en.html
49. Nystrom, A. M., and Fadeel, B. (2012) Safety assessment of nanomaterials: Implications for nanomedicine, *J. Controlled Release* 161, 403-408.
 50. European Commission, Brussels (2005) Communication from the commission to the council, the European parliament and the economic and social committee. Nanosciences and nanotechnologies: An action plan for Europe 2005-2009, can be downloaded from http://ec.europa.eu/nanotechnology/policies_en.html
 51. European Commission, Brussels (2007) Communication from the commission to the council, the European parliament and the European economic and social committee. Nanosciences and Nanotechnologies: An action plan for Europe 2005-2009. First Implementation Report 2005-2007, can be downloaded from http://ec.europa.eu/nanotechnology/policies_en.html
 52. European Commission, Brussels (2009) Communication from the commission to the council, the European parliament and the European economic and social committee. Nanosciences and Nanotechnologies: An action plan for Europe 2005-2009. Second Implementation Report 2007-2009, can be downloaded from http://ec.europa.eu/nanotechnology/policies_en.html
 53. Kemikalieinspektionen, Sundbyberg (2010) Säker användning av nanomaterial. Behov av reglering och andra åtgärder – rapport från ett regeringsuppdrag, can be downloaded from <http://www.kemi.se>
 54. Moghimi, S. M., Hunter, A. C., and Murray, J. C. (2005) Nanomedicine: current status and future prospects, *Faseb Journal* 19, 311-330.
 55. Allen, T. M., and Cullis, P. R. (2004) Drug delivery systems: Entering the mainstream, *Science* 303, 1818-1822.
 56. Frangioni, J. V. (2003) In vivo near-infrared fluorescence imaging, *Curr. Opin. Chem. Biol.* 7, 626-634.
 57. Jain, K. K. (2005) Nanotechnology in clinical laboratory diagnostics, *Clinica Chimica Acta* 358, 37-54.
 58. Liu, H., and Webster, T. J. (2007) Nanomedicine for implants: A review of studies and necessary experimental tools, *Biomaterials* 28, 354-369.
 59. Chan, W. C. W. (2007) *Bio-applications of nanoparticles*, Springer Science, New York.
 60. Torchilin, V. P. (2006) *Nanoparticulates as drug carriers*, Imperial Collage Press, London.
 61. Laqueur, E., and Grevenstuck, A. (1924) Über die Wirkung Intratrachealer Zuführung von Insulin, *Klinische Wochenschrift* 3, 1273-1274.
 62. Owens, D. R., Zinman, B., and Bolli, G. (2003) Alternative routes of insulin delivery, *Diabetic Medicine* 20, 886-898.
 63. Siekmeier, R., and Scheuch, G. (2008) Inhaled insulin - does it become reality?, *Journal of Physiology and Pharmacology* 59, 81-113.
 64. Mack, G. S. (2007) Pfizer dumps Exubera, *Nat. Biotechnol.* 25, 1331-1332.
 65. Morishita, M., Goto, T., Nakamura, K., Lowman, A. M., Takayama, K., and Peppas, N. A. (2006) Novel oral insulin delivery systems based on complexation polymer hydrogels: Single and multiple administration studies in type 1 and 2 diabetic rats, *J. Controlled Release* 110, 587-594.

66. Mesiha, M. S., Sidhom, M. B., and Fasipe, B. (2005) Oral and subcutaneous absorption of insulin poly(isobutylycyanoacrylate) nanoparticles, *Int. J. Pharm.* 288, 289-293.
67. Degim, I. T., Gumusel, B., Degim, Z., Ozcelikay, T., Tay, A., and Guner, S. (2006) Oral administration of liposomal insulin, *Journal of Nanoscience and Nanotechnology* 6, 2945-2949.
68. Sarmiento, B., Ribeiro, A., Veiga, F., Sampaio, P., Neufeld, R., and Ferreira, D. (2007) Alginate/Chitosan nanoparticles are effective for oral insulin delivery, *Pharmaceutical Research* 24, 2198-2206.
69. Mao, S. R., Bakowsky, U., Jintapattanakit, A., and Kissel, T. (2006) Self-assembled polyelectrolyte nanocomplexes between chitosan derivatives and insulin, *J. Pharm. Sci.* 95, 1035-1048.
70. Park, W., and Na, K. (2009) Polyelectrolyte complex of chondroitin sulfate and peptide with lower pI value in poly(lactide-co-glycolide) microsphere for stability and controlled release, *Colloids Surf. B Biointerfaces* 72, 193-200.
71. Mendelsohn, J., and Baselga, J. (2006) Epidermal Growth Factor Receptor Targeting in Cancer, *Semin. Oncol.* 33, 369-385.
72. Maeda, H., Wu, J., Sawa, T., Matsumura, Y., and Hori, K. (2000) Tumor vascular permeability and the EPR effect in macromolecular therapeutics: a review, *J. Controlled Release* 65, 271-284.
73. Serksen, S. R., Westcott, S. L., Halas, N. J., and West, J. L. (2000) Temperature-sensitive polymer-nanoshell composites for photothermally modulated drug delivery, *Journal of Biomedical Materials Research* 51, 293-298.
74. Davidsen, J., Jorgensen, K., Andresen, T. L., and Mouritsen, O. G. (2003) Secreted phospholipase A(2) as a new enzymatic trigger mechanism for localised liposomal drug release and absorption in diseased tissue, *Biochimica Et Biophysica Acta-Biomembranes* 1609, 95-101.
75. Sethuraman, V. A., Lee, M. C., and Bae, Y. H. (2008) A biodegradable pH-sensitive micelle system for targeting acidic solid tumors, *Pharmaceutical Research* 25, 657-666.
76. Harris, J. M., and Chess, R. B. (2003) Effect of pegylation on pharmaceuticals, *Nature Reviews Drug Discovery* 2, 214-221.
77. Owens Iii, D. E., and Peppas, N. A. (2006) Opsonization, biodistribution, and pharmacokinetics of polymeric nanoparticles, *Int. J. Pharm.* 307, 93-102.
78. Vogel, V. (2009) *Nanotechnology. Vol. 5, Nanomedicine*, Wiley-VCH, Weinheim.
79. Duncan, R. (2003) The dawning era of polymer therapeutics, *Nature Reviews Drug Discovery* 2, 347-360.
80. Hartig, S. M., Greene, R. R., Dikov, M. M., Prokop, A., and Davidson, J. M. (2007) Multifunctional nanoparticulate polyelectrolyte complexes, *Pharmaceutical Research* 24, 2353-2369.
81. Shu, S., Zhang, X., Teng, D., Wang, Z., and Li, C. (2009) Polyelectrolyte nanoparticles based on water-soluble chitosan-poly(l-aspartic acid)-polyethylene glycol for controlled protein release, *Carbohydrate Research* 344, 1197-1204.

82. Schatz, C., Lucas, J. M., Viton, C., Domard, A., Pichot, C., and Delair, T. (2004) Formation and properties of positively charged colloids based on polyelectrolyte complexes of biopolymers, *Langmuir* **20**, 7766-7778.
83. Luppi, B., Bigucci, F., Mercolini, L., Musenga, A., Sorrenti, M., Catenacci, L., and Zecchi, V. (2009) Novel mucoadhesive nasal inserts based on chitosan/hyaluronite polyelectrolyte complexes for peptide and protein delivery, *J. Pharm. Pharmacol.* **61**, 151-157.
84. Piroton, S., Muller, C., Pantoustier, N., Botteman, F., Collinet, B., Grandfils, C., Dandrifosse, G., Degee, P., Dubois, P., and Raes, M. (2004) Enhancement of transfection efficiency through rapid and noncovalent post-PEGylation of poly(dimethylaminoethyl methacrylate)/DNA complexes, *Pharmaceutical Research* **21**, 1471-1479.
85. Lin, C., Zhong, Z. Y., Lok, M. C., Jiang, X. L., Hennink, W. E., Feijen, J., and Engbersen, J. F. J. (2007) Novel bioreducible poly(amido amine)s for highly efficient gene delivery, *Bioconj. Chem.* **18**, 138-145.
86. Arruebo, M., Fernandez-Pacheco, R., Ibarra, M. R., and Santamaria, J. (2007) Magnetic nanoparticles for drug delivery, *Nano Today* **2**, 22-32.
87. Alexiou, C., Jurgons, R., Seliger, G., and Iro, H. (2006) Medical applications of magnetic nanoparticles, *Journal of Nanoscience and Nanotechnology* **6**, 2762-2768.
88. Tan, S., Tan, H. T., and Chung, M. C. M. (2008) Membrane proteins and membrane proteomics, *Proteomics* **8**, 3924-3932.
89. Singer, S. J., and Nicolson, G. L. (1972) The Fluid Mosaic Model of the Structure of Cell Membranes, *Science* **175**, 720-731.
90. Kusumi, A., Fujiwara, T. K., Morone, N., Yoshida, K. J., Chadda, R., Xie, M., Kasai, R. S., and Suzuki, K. G. N. (2012) Membrane mechanisms for signal transduction: The coupling of the meso-scale raft domains to membrane-skeleton-induced compartments and dynamic protein complexes, *Semin. Cell Dev. Biol.* **23**, 126-144.
91. Brown, D. A., and London, E. (2000) Structure and function of sphingolipid- and cholesterol-rich membrane rafts, *J. Biol. Chem.* **275**, 17221-17224.
92. Hopkins, A. L., and Groom, C. R. (2002) The druggable genome, *Nat Rev Drug Discov* **1**, 727-730.
93. Sud, M., Fahy, E., Cotter, D., Brown, A., Dennis, E. A., Glass, C. K., Merrill, A. H., Murphy, R. C., Raetz, C. R. H., Russell, D. W., and Subramaniam, S. (2007) LMSD: LIPID MAPS structure database, *Nucleic Acids Res.* **35**, D527-D532.
94. van Meer, G., Voelker, D. R., and Feigenson, G. W. (2008) Membrane lipids: where they are and how they behave, *Nature Reviews Molecular Cell Biology* **9**, 112-124.
95. Zhdanov, R. I., Podobed, O. V., and Vlassov, V. V. (2002) Cationic lipid-DNA complexes-lipoplexes-for gene transfer and therapy, *Bioelectrochemistry* **58**, 53-64.
96. Sahay, G., Alakhova, D. Y., and Kabanov, A. V. (2010) Endocytosis of nanomedicines, *J. Controlled Release* **145**, 182-195.
97. Harush-Frenkel, O., Debotton, N., Benita, S., and Altschuler, Y. (2007) Targeting of nanoparticles to the clathrin-mediated endocytic pathway, *Biochem. Biophys. Res. Commun.* **353**, 26-32.

98. Harush-Frenkel, O., Rozentur, E., Benita, S., and Altschuler, Y. (2008) Surface charge of nanoparticles determines their endocytic and transcytotic pathway in polarized MDCK cells, *Biomacromolecules* 9, 435-443.
99. Chithrani, B. D., Ghazani, A. A., and Chan, W. C. W. (2006) Determining the size and shape dependence of gold nanoparticle uptake into mammalian cells, *Nano Lett.* 6, 662-668.
100. Osaki, F., Kanamori, T., Sando, S., Sera, T., and Aoyama, Y. (2004) A quantum dot conjugated sugar ball and its cellular uptake on the size effects of endocytosis in the subviral region, *J. Am. Chem. Soc.* 126, 6520-6521.
101. Li, X. L. (2012) Size and shape effects on receptor-mediated endocytosis of nanoparticles, *J. Appl. Phys.* 111.
102. Carver, L. A., and Schnitzer, J. E. (2003) Caveolae: Mining little caves for new cancer targets, *Nature Reviews Cancer* 3, 571-581.
103. Rejman, J., Conese, M., and Hoekstra, D. (2006) Gene transfer by means of lipo- and polyplexes: Role of clathrin and caveolae-mediated endocytosis, *J. Liposome Res.* 16, 237-247.
104. Oh, P., Borgstrom, P., Witkiewicz, H., Li, Y., Borgstrom, B. J., Chrastina, A., Iwata, K., Zinn, K. R., Baldwin, R., Testa, J. E., and Schnitzer, J. E. (2007) Live dynamic imaging of caveolae pumping targeted antibody rapidly and specifically across endothelium in the lung, *Nature Biotechnology* 25, 327-337.
105. Sessa, G., and Weissmann, G. (1968) Phospholipid spherules (liposomes) as a model for biological membranes, *J. Lipid Res.* 9, 310-318.
106. Hope, M. J., Bally, M. B., Webb, G., and Cullis, P. R. (1985) Production of large unilamellar vesicles by a rapid extrusion procedure. Characterization of size distribution, trapped volume and ability to maintain a membrane potential, *Biochimica Et Biophysica Acta* 812, 55-65.
107. MacDonald, R. C., MacDonald, R. I., Menco, B. P. M., Takeshita, K., Subbarao, N. K., and Hu, L.-r. (1991) Small-volume extrusion apparatus for preparation of large, unilamellar vesicles, *Biochimica et Biophysica Acta (BBA) - Biomembranes* 1061, 297-303.
108. Richter, R. P., Bérat, R., and Brisson, A. R. (2006) Formation of solid-supported lipid bilayers: An integrated view, *Langmuir* 22, 3497-3505.
109. Reimhult, E., Höök, F., and Kasemo, B. (2003) Intact vesicle adsorption and supported biomembrane formation from vesicles in solution: Influence of surface chemistry, vesicle size, temperature, and osmotic pressure, *Langmuir* 19, 1681-1691.
110. Thid, D., Benkoski, J. J., Svedhem, S., Kasemo, B., and Gold, J. (2007) DHA-induced changes of supported lipid membrane morphology, *Langmuir* 23, 5878-5881.
111. Tanaka, M., and Sackmann, E. (2005) Polymer-supported membranes as models of the cell surface, *Nature* 437, 656-663.
112. Sackmann, E., and Tanaka, M. (2000) Supported membranes on soft polymer cushions: fabrication, characterization and applications, *Trends Biotechnol.* 18, 58-64.
113. Sinner, E. K., and Knoll, W. (2001) Functional tethered membranes, *Curr. Opin. Chem. Biol.* 5, 705-711.

114. Hong, S., Hessler, J. A., Banaszak Holl, M. M., Leroueil, P., Mecke, A., and Orr, B. G. (2006) Physical interactions of nanoparticles with biological membranes: The observation of nanoscale hole formation, *Journal of Chemical Health and Safety* 13, 16-20.
115. Edvardsson, M., Svedhem, S., Wang, G., Richter, R., Rodahl, M., and Kasemo, B. (2009) QCM-D and Reflectometry Instrument: Applications to Supported Lipid Structures and Their Biomolecular Interactions, *Anal. Chem.* 81, 349-361.
116. Zasadzinski, J. A., Viswanthan, R., Madsen, L., Garnaes, J., and Schwartz, D. K. (1994) Langmuir-Blodgett Films, *Science* 263, 1726-1733.
117. Peetla, C., Stine, A., and Labhasetwar, V. (2009) Biophysical Interactions with Model Lipid Membranes: Applications in Drug Discovery and Drug Delivery, *Molecular Pharmaceutics* 6, 1264-1276.
118. Brockman, H. (1999) Lipid monolayers: Why use half a membrane to characterize protein-membrane interactions?, *Current Opinion in Structural Biology* 9, 438-443.
119. Ihalainen, P., and Peltonen, J. (2002) Covalent Immobilization of Antibody Fragments onto Langmuir-Schaefer Binary Monolayers Chemisorbed on Gold, *Langmuir* 18, 4953-4962.
120. Israelachvili, J. N. (2011) *Intermolecular and Surface Forces (Third Edition)*, Academic Press, San Diego.
121. Gref, R., Luck, M., Quellec, P., Marchand, M., Dellacherie, E., Harnisch, S., Blunk, T., and Muller, R. H. (2000) 'Stealth' corona-core nanoparticles surface modified by polyethylene glycol (PEG): influences of the corona (PEG chain length and surface density) and of the core composition on phagocytic uptake and plasma protein adsorption, *Colloids Surf. B Biointerfaces* 18, 301-313.
122. Min, Y. J., Akbulut, M., Kristiansen, K., Golan, Y., and Israelachvili, J. (2008) The role of interparticle and external forces in nanoparticle assembly, *Nat. Mater.* 7, 527-538.
123. Nel, A. E., Madler, L., Velegol, D., Xia, T., Hoek, E. M. V., Somasundaran, P., Klaessig, F., Castranova, V., and Thompson, M. (2009) Understanding biophysicochemical interactions at the nano-bio interface, *Nat. Mater.* 8, 543-557.
124. Lynch, I., and Dawson, K. A. (2008) Protein-nanoparticle interactions, *Nano Today* 3, 40-47.
125. Walczyk, D., Bombelli, F. B., Monopoli, M. P., Lynch, I., and Dawson, K. A. (2010) What the Cell "Sees" in Bionanoscience, *J. Am. Chem. Soc.* 132, 5761-5768.
126. Cedervall, T., Lynch, I., Lindman, S., Berggard, T., Thulin, E., Nilsson, H., Dawson, K. A., and Linse, S. (2007) Understanding the nanoparticle-protein corona using methods to quantify exchange rates and affinities of proteins for nanoparticles, *Proc. Natl. Acad. Sci. U. S. A.* 104, 2050-2055.
127. Lundqvist, M., Stigler, J., Elia, G., Lynch, I., Cedervall, T., and Dawson, K. A. (2008) Nanoparticle size and surface properties determine the protein corona with possible implications for biological impacts, *Proc. Natl. Acad. Sci. U. S. A.* 105, 14265-14270.

128. Lewinski, N., Colvin, V., and Drezek, R. (2008) Cytotoxicity of nanoparticles, *Small* 4, 26-49.
129. Haslam, G., Wyatt, D., and Kitos, P. A. (2000) Estimating the number of viable animal cells in multi-well cultures based on their lactate dehydrogenase activities, *Cytotechnology* 32, 63-75.
130. Mosmann, T. (1983) Rapid colorimetric assay for cellular growth and survival - application to proliferation and cyto-toxicity assays, *J. Immunol. Methods* 65, 55-63.
131. Levi, V., Serpinskaya, A. S., Gratton, E., and Gelfand, V. (2006) Organelle transport along microtubules in *Xenopus melanophores*: Evidence for cooperation between multiple motors, *Biophys. J.* 90, 318-327.
132. Aspengren, S., Skold, H. N., and Wallin, M. (2009) Different strategies for color change, *Cell. Mol. Life Sci.* 66, 187-191.
133. Aspengren, S., Hedberg, D., and Wallin, M. (2007) Melanophores: A model system for neuronal transport and exocytosis?, *J. Neurosci. Res.* 85, 2591-2600.
134. Gross, S. P., Tuma, M. C., Deacon, S. W., Serpinskaya, A. S., Reilein, A. R., and Gelfand, V. I. (2002) Interactions and regulation of molecular motors in *Xenopus melanophores*, *J. Cell Biol.* 156, 855-865.
135. Levi, V., Gelfand, V. I., Serpinskaya, A. S., and Gratton, E. (2006) Melanosomes transported by myosin-V in *Xenopus melanophores* perform slow 35 nm steps, *Biophys. J.* 90, L7-L9.
136. Aspengren, S., Wielbass, L., and Wallin, M. (2006) Effects of acrylamide, latrunculin, and nocodazole on intracellular transport and cytoskeletal organization in melanophores, *Cell Motil. Cytoskeleton* 63, 423-436.
137. Kaszuba, M., McKnight, D., Connah, M. T., McNeil-Watson, F. K., and Nobbmann, U. (2008) Measuring sub nanometre sizes using dynamic light scattering, *Journal of Nanoparticle Research* 10, 823-829.
138. Kaszuba, M., Connah, M. T., McNeil-Watson, F. K., and Nobbmann, U. (2007) Resolving concentrated particle size mixtures using dynamic light scattering, *Particle & Particle Systems Characterization* 24, 159-162.
139. Keller, C. A., and Kasemo, B. (1998) Surface specific kinetics of lipid vesicle adsorption measured with a quartz crystal microbalance, *Biophys. J.* 75, 1397-1402.
140. Glasmaster, K., Larsson, C., Hook, F., and Kasemo, B. (2002) Protein adsorption on supported phospholipid bilayers, *J. Colloid Interface Sci.* 246, 40-47.
141. Janshoff, A., Galla, H. J., and Steinem, C. (2000) Piezoelectric mass-sensing devices as biosensors - An alternative to optical biosensors?, *Angew. Chem. Int. Ed.* 39, 4004-4032.
142. Sauerbrey, G. (1959) Verwendung von Schwingquartzen zur Wagung Dunner Schichten und zur Mikrowagung, *Zeitschrift Fur Physik* 155, 206-222.
143. Rodahl, M., Höök, F., Krozer, A., Brzezinski, P., and Kasemo, B. (1995) Quartz-crystal microbalance setup for frequency and Q-factor measurements in gaseous and liquid environments, *Review of Scientific Instruments* 66, 3924-3930.

144. Kanazawa, K. K., and Gordon, J. G. (1985) Frequency of a quartz microbalance in contact with liquid, *Anal. Chem.* *57*, 1770-1771.
145. Cooper, M. A., and Singleton, V. T. (2007) A survey of the 2001 to 2005 quartz crystal microbalance biosensor literature: applications of acoustic physics to the analysis of biomolecular interactions, *J. Mol. Recognit.* *20*, 154-184.
146. Becker, B., and Cooper, M. A. (2011) A survey of the 2006-2009 quartz crystal microbalance biosensor literature, *J. Mol. Recognit.* *24*, 754-787.
147. Heitmann, V., and Wegener, J. (2007) Monitoring cell adhesion by piezoresonators: Impact of increasing oscillation amplitudes, *Anal. Chem.* *79*, 3392-3400.
148. Knerr, R., Weiser, B., Drotleff, S., Steinem, C., and Gopferich, A. (2006) Measuring cell adhesion on RGD-modified, self-assembled PEG monolayers using the quartz crystal microbalance technique, *Macromol. Biosci.* *6*, 827-838.
149. Saitakis, M., Tsortos, A., and Gizeli, E. (2010) Probing the interaction of a membrane receptor with a surface-attached ligand using whole cells on acoustic biosensors, *Biosens. Bioelectron.* *25*, 1688-1693.
150. Tymchenko, N., Nilebäck, E., Voinova, M. V., Gold, J., Kasemo, B., and Svedhem, S. (2012) Reversible Changes in Cell Morphology due to Cytoskeletal Rearrangements Measured in Real-Time by QCM-D, *Biointerphases* *7*.
151. Marx, K. A., Zhou, T., Montrone, A., McIntosh, D., and Braunhut, S. J. (2007) A comparative study of the cytoskeleton binding drugs nocodazole and taxol with a mammalian cell quartz crystal microbalance biosensor: Different dynamic responses and energy dissipation effects, *Anal. Biochem.* *361*, 77-92.
152. Heitmann, V., Reiß, B., and Wegener, J. (2007) The quartz crystal microbalance in cell biology: basics and applications, In *Piezoelectric Sensors* (Steinem, C., and Janshoff, A., Eds.), pp 303-338, Springer-Verlag, Heidelberg.
153. Cans, A. S., Hook, F., Shupliakov, O., Ewing, A. G., Eriksson, P. S., Brodin, L., and Orwar, O. (2001) Measurement of the dynamics of exocytosis and vesicle retrieval at cell populations using a quartz crystal microbalance, *Anal. Chem.* *73*, 5805-5811.
154. Ingber, D. E. (2003) Tensegrity I. Cell structure and hierarchical systems biology, *J. Cell Sci.* *116*, 1157-1173.
155. Fuller, B. (1961) Tensegrity, *Portfolio and Art News Annual* *4*, 112-127.
156. Wang, G., Dewilde, A. H., Zhang, J. P., Pal, A., Vashist, M., Bello, D., Marx, K. A., Braunhut, S. J., and Therrien, J. M. (2011) A living cell quartz crystal microbalance biosensor for continuous monitoring of cytotoxic responses of macrophages to single-walled carbon nanotubes, *Particle and Fibre Toxicology* *8*.
157. Colton, R. J., Baselt, D. R., Dufrene, Y. F., Green, J. B. D., and Lee, G. U. (1997) Scanning probe microscopy, *Curr. Opin. Chem. Biol.* *1*, 370-377.
158. Cohen, S. R., and Bitler, A. (2008) Use of AFM in bio-related systems, *Current Opinion in Colloid & Interface Science* *13*, 316-325.
159. Cross, G. H., Reeves, A. A., Brand, S., Popplewell, J. F., Peel, L. L., Swann, M. J., and Freeman, N. J. (2003) A new quantitative optical biosensor for protein characterisation, *Biosens. Bioelectron.* *19*, 383-390.

160. Swann, M. J., Peel, L. L., Carrington, S., and Freeman, N. J. (2004) Dual-polarization interferometry: an analytical technique to measure changes in protein structure in real time, to determine the stoichiometry of binding events, and to differentiate between specific and nonspecific interactions, *Anal. Biochem.* **329**, 190-198.
161. Terry, C. J., Popplewell, J. F., Swann, M. J., Freeman, N. J., and Fernig, D. G. (2006) Characterisation of membrane mimetics on a dual polarisation interferometer, *Biosens. Bioelectron.* **22**, 627-632.
162. Mashaghi, A., Swann, M., Popplewell, J., Textor, M., and Reimhult, E. (2008) Optical anisotropy of supported lipid structures probed by waveguide spectroscopy and its application to study of supported lipid bilayer formation kinetics, *Anal. Chem.* **80**, 3666-3676.
163. Wang, G., Rodahl, M., Edvardsson, M., Svedhem, S., Ohlsson, G., Höök, F., and Kasemo, B. (2008) A combined reflectometry and quartz crystal microbalance with dissipation setup for surface interaction studies, *Review of Scientific Instruments* **79**.
164. Verma, A., and Stellacci, F. (2010) Effect of Surface Properties on Nanoparticle-Cell Interactions, *Small* **6**, 12-21.
165. Yang, K., and Ma, Y. Q. (2010) Computer simulation of the translocation of nanoparticles with different shapes across a lipid bilayer, *Nat. Nanotechnol.* **5**, 579-583.
166. Schulz, M., Olubummo, A., and Binder, W. H. (2012) Beyond the lipid-bilayer: interaction of polymers and nanoparticles with membranes, *Soft Matter* **8**, 4849-4864.
167. Lin, C., and Engbersen, J. F. J. (2009) The role of the disulfide group in disulfide-based polymeric gene carriers, *Expert Opinion on Drug Delivery* **6**, 421-439.
168. Abbas, Z., Holmberg, J. P., Hellstrom, A. K., Hagstrom, M., Bergenholtz, J., Hasselov, M., and Ahlberg, E. (2011) Synthesis, characterization and particle size distribution of TiO₂ colloidal nanoparticles, *Colloids and Surfaces a-Physicochemical and Engineering Aspects* **384**, 254-261.
169. Donaldson, K., Murphy, F., Schinwald, A., Duffin, R., and Poland, C. A. (2011) Identifying the pulmonary hazard of high aspect ratio nanoparticles to enable their safety-by-design, *Nanomedicine* **6**, 143-156.

